Neural Computing and Applications (2023) 35:4027–4049
https://doi.org/10.1007/s00521-022-07865-3

ORIGINAL ARTICLE

Disturbance-observer-based adaptive dynamic surface control for nonlinear systems with input dead-zone and delay using neural networks

Junchang Zhai[1] · Huanqing Wang[1] · Jiaqing Tao[1]

Received: 17 March 2022 / Accepted: 21 September 2022 / Published online: 19 October 2022

Abstract
Disturbance-observer-based adaptive neural control approach is proposed for nonlinear systems. Considering the effect caused by long input delay and dead-zone, a novel auxiliary system has been introduced to degrade the design difficult. Based on the auxiliary system, a novel disturbance observer is developed to estimate the unknown time-varying external disturbance and the approximation error. What is more, the priori knowledge on the boundary of the disturbance and approximation error is not required for the disturbance observer. The "explosion of complexity" problem has been overcome by using dynamic surface control (DSC) scheme. By combing DSC scheme with backstepping technique, an adaptive neural dynamic surface controller is correctly devised to improve the disturbance rejection performance of the closed-loop system. Finally, the simulations of two examples show the superiority of the proposed scheme.

Keywords Neural networks · Dynamic surface control · Backstepping · Input delay · Disturbance observer

1 Introduction

Over the past years, many meaningful results have been proposed for nonlinear systems control in [1–3]. However, most of these results are obtained on the premise that the uncertain nonlinearity in system are known or bounded by known nonlinear functions. It should be pointed out that this assumption is not applicable to practical applications, because it is difficult to get the accurate system model or the information of the nonlinear term in practice. To overcome this drawback, the neural networks (NNS) and fuzzy logic systems (FLS) are introduced to construct the adaptive controller by combing the adaptive backstepping method in [4–10]. However, in the process of backstepping design, the "explosion of complexity" increases sharply with repeating differentiation of the virtual controller in the aforementioned results. Thus, the DSC scheme was proposed in [11] and many meaningful research results have been developed for strict-feedback nonlinear systems in [12–17]. However, some common phenomena such as external disturbance [18, 19], time delay [20, 21] and non-smooth nonlinearity [22, 23] bring great challenges to the controller design of strict-feedback nonlinear systems.

In general, many actual systems often suffer from different external disturbances. These disturbances are usually time-varying and unknown. As a result, it is difficult to obtain their accurate information, and the difficulty of system control increases sharply. The disturbance can break the control performance of the closed-loop system and even lead to disastrous results. Thus it is necessary to consider the external disturbance rejection performance of the closed-loop system. The authors in [24] first proposed the disturbance-observer-based control (DOBC) strategy. Unlike the general adaptive control approach, the disturbance observer (DO) can estimate the external disturbance and provide valuable information for control law design. Consequently, the robustness of the closed-loop system is improved effectively by using DOBC strategy. Inspired by the idea of DOBC, [25–27] proposed adaptive sliding terminal control scheme for strict-feedback nonlinear systems. Furthermore, considering mismatched disturbances, [28–30] proposed the disturbance rejection scheme for

✉ Junchang Zhai
zhaijunchang@bhu.edu.cn

[1] College of Mathetatical Science, Bohai University, Jinzhou 121013, Liaoning, China

nonlinear systems. Recently, based on DOBC [31–33] proposed adaptive neural/fuzzy control for strict-feedback nonlinear systems, respectively. It should be noted that the imperfections are unavoidable in the practical production processes [34]. For instance, the authors in [35] proposed a control scheme for imperfect electromechanical round system. Furthermore, an optimal control approach for imperfect electronic circuits system was considered in [36]. Although the real devices still operate well in regimes far from ideality, the usual control approaches may useless. In addition, the dead-zone problem has not been considered in the aforementioned results. In contrast to time-varying external disturbance, the input dead-zone is a typical non-smooth nonlinearity problem, which often occurs in many physical components of control systems [37]. However, the control forces provided by the actuators are limited in practice. Thus, the output provided by the disturbance observer cannot be effective utilized by the control signal when the input dead-zone appears. As a result, the closed-loop systems will be unstable or even disastrous if the input dead-zone is ignored. Recently, in order to solve the problem of dead-zone in nonlinear systems, many meaningful results have been developed by the researchers in [38–41]. Although the input dead-zone problem has been widely studied by the researchers, these issues rarely considered in the DOBC scheme. In addition, the control schemes proposed in the aforementioned results cannot be extended to strict-feedback nonlinear systems with unknown time-varying external disturbance and input dead-zone.

On the other hand, as a kind of time delay, input delay is a common and inevitable phenomenon in practical control systems [42–44]. When input delay occurs, the performance of the closed-loop system will be damaged or even be disastrous if the control signal cannot feedback the information provided by the observer in time. However, the traditional state delay control methods proposed in [45–47] cannot be directly used to solve input delay. For nonlinear systems with input delay, the authors in [48] extended the predictor-based control approach to tackle input delay. However, for the predictor-based control method, the state of system is difficult to predict. In recent years, based on FLS and the idea of Pade approximation, [49] considered input delay and output constraint for strict-feedback nonlinear systems. Furthermore, considering strict-feedback nonlinear with state constrained and input delay, [50] proposed an adaptive tracking control approach by combing Pade approximation and NNS with adaptive backstepping technique. Later, the authors in [51, 52] developed a compensation mechanism or combing compensation mechanism with Pade approximation to degrade the effect of the input delay. Nevertheless, the Pade approximation approach is invalid for long input delay. In addition, most of existing results are invalid for strict-feedback nonlinear systems with time-varying external disturbance, input delay and dead-zone, simultaneously. Recently, [53] considered the input saturation, input delay and external disturbance for state constrained strict-feedback nonlinear systems. Unfortunately, if the long input delay or the dead-zone problem occurs the proposed method in [53] is invalid. Since input dead-zone and input delay are common phenomena in practical systems, the disturbance rejection ability is more in line with the robust performance requirements of the closed-loop system, it is a significant issue to consider strict-feedback nonlinear systems with time-varying external disturbance, input dead-zone and input delay. However, the aforementioned results cannot be directly generalized to this issue, which prompted us to carry out our research.

The aforementioned observation motivates us to discuss disturbance-observer-based adaptive neural dynamic surface control for strict-feedback nonlinear systems with time-varying external disturbance, input dead-zone and input delay. The main work of this paper is listed as follows:

(1) Taking into account the effect caused by long input delay and dead-zone, a novel auxiliary system is introduced for the first time to degrade the design difficulty in each step. Compared with [49–53] the proposed method can tackle the long input delay.
(2) DSC is introduced to tackle the "explosion of complexity" problem in each backstepping step, which can reduce the burden of computation. The radial basis function neural networks are introduced to approximate the unknown nonlinear functions.
(3) Based on the proposed auxiliary system, a novel adaptive disturbance observer is introduced for the first time to estimate the unknown time-varying external disturbance and approximation error in each backstepping step. Unlike the usual disturbance observer, the boundary information of the time-varying external disturbance or approximate error is not required for the disturbance observer design. Compared with [28–33], the proposed method which not only estimates the unknown time-varying external disturbance and the approximation error caused by the NNS, but also eliminates the effect caused by input delay and dead zone. Furthermore, the closed-loop systems show better robust performance.

The reminder of this paper is organized as follows: Section 2 presents the problem and the preliminary results. Section 3 discusses the design process of the controller and the stability analysis. The simulation examples are considered in Sect. 4. Finally, a brief conclusion is given in Sect. 5.

2 Preliminary

2.1 Problem formulation

Consider the strict-feedback nonlinear system as

$$\begin{cases} \dot{x}_i(t) = f_i(\bar{x}_i(t)) + x_{i+1}(t) + d_i(t), & 1 \le i \le n-1 \\ \dot{x}_n(t) = f_n(\bar{x}_n(t)) + D(v(t-\tau)) + d_n(t) \\ y(t) = x_1(t) \end{cases} \tag{1}$$

where the state variable $\bar{x}_i(t) = [x_1(t), x_2(t), \cdots, x_i(t)]^T \in R^i, i = 1, 2, \cdots, n$, $D(v(t-\tau)) \in R$ denotes the control input with input dead-zone and delay, where τ represents the known constant or time-varying input delay, the system output $y(t) \in R$. For $1 \le i \le n$, $f_i(\cdot)$ is unknown smooth nonlinear function, $d_i(t)$ represents the unknown and time-varying external disturbance.

According to [38], $D(v(t))$ is defined as

$$D(v(t)) = \begin{cases} m_r(v(t) - b_r), & v(t) \ge b_r \\ 0\ , & b_l < v(t) < b_r \\ m_l(v(t) - b_l), & v(t) \le b_l \end{cases} \tag{2}$$

where $v(t) \in R$ denotes the input to the dead-zone, and $D(.)$ denotes the output to the dead-zone.

Assumption 1 [38]: The dead-zone slopes $m_r = m_l = m$.

Assumption 2 [38]: The parameters m, b_r and b_l in (2) are bounded, i.e., $m_{min} < m < m_{max}$, $b_{r_{\min}} < b_r < b_{r_{\max}}$ and $b_{l_{\min}} < b_l < b_{l_{\max}}$ with m_{min}, m_{max}, $b_{r_{\min}}$, $b_{r_{\max}}$, $b_{l_{\min}}$ and $b_{l_{\max}}$ being known constants.

Assumption 3 [38]: The signs for m, b_r and b_l are known, i.e., $m > 0$, $b_r > 0$, $b_l < 0$.

Then, we redefine (2) as

$$D(v(t)) = mv(t) + d(v(t)) \tag{3}$$

where

$$d(v(t)) = \begin{cases} -mb_r, & v(t) \ge b_r \\ -mv(t), & b_l < v(t) < b_r \\ -mb_l, & v(t) \le b_l \end{cases} \tag{4}$$

Based on Assumptions 1 and 2, the term $d(v(t))$ is bounded, i.e., $|d(v(t))| \le d^*$, with $d^* = max\{mb_r, -mb_l\}$.

Remark 1 In practice, many systems can be described or transform as the system (1), such as liquid level control system [53], power systems [54], maglev suspension systems [55, 56], and so on.

Remark 2 Compared with the works in [28–33] which only considered external disturbance, the effect of input dead-zone and input delay was unconsidered. Compared with the works in [49–53] which only focus on strict-feedback nonlinear systems with input delay, however, the effect of input dead-zone and the disturbance rejection ability of the closed-loop system are ignored. In addition, the developed method in [49–53] cannot work in long input delay.

The main idea of this research is to establish a unified framework of disturbance-observer-based adaptive neural dynamic surface control scheme for strict-feedback nonlinear systems with time-varying external disturbance, input dead-zone and input delay. Furthermore, the proposed controller can show effective tracking performance for the reference signal $y_d(t)$ and the closed-loop system shows better disturbance rejection performance.

Assumption 4 For $1 \le i \le n$, the unknown time-varying external disturbances $d_i(t)$ and its derivative $\dot{d}_i(t)$ satisfy $|d_i(t)| \le \bar{d}_{iU}$ and $|\dot{d}_i(t)| \le \bar{d}_{iD}$, where $\bar{d}_{iU}$ and $\bar{d}_{iD}$ are unknown positive constants.

Assumption 5 [57]: The reference trajectory $y_d(t)$ and its time derivatives $\ddot{y}_d(t)$ are bounded, i.e., $\Theta_0 := \{(y_d, \dot{y}_d, \ddot{y}_d) : (y_d)^2 + (\dot{y}_d)^2 + (\ddot{y}_d)^2 \le B_0\}$, where B_0 is a positive constant.

2.2 Neural networks

In the process of controller design, the NNS are used to approximate the unknown nonlinear function $f(Z) : R^n \to R$. Assume that l represents the number of nodes in NNS, then $f(Z)$ can be modeled by

$$f_{nn}(Z) = W^T \Phi(Z) \tag{5}$$

For Eq. (5), Z represents the input vector and $Z \in \Omega_z \subset R^q$. $W \in R^l$ represents the weight vector and $W = [w_1, w_2, ..., w_l]^T$. $\Phi(Z) = [s_1(Z), s_2(Z), ..., s_l(Z)]^T \in R^l$ is the basis function vector with $s_i(Z)$ $(i = 1, 2, \cdots, l)$ being the Gaussian-like function, i.e.,

$$s_i(Z) = \exp\left[-\frac{(Z - v_i)^T (Z - v_i)}{\eta^2}\right] \tag{6}$$

where η represents the width of the Gaussian function, and $v_i = [v_{i1}, v_{i2}, ..., v_{iq}]^T$ denotes the center of the receptive domain.

For $f(Z)$ defined on a compact set Ω_Z, according to literature [7], there exists a suitable $W^{*T}\Phi(Z)$ which satisfies

$$f(Z) = W^{*T}\Phi(Z) + \delta(Z), \quad \forall z \in \Omega_Z \tag{7}$$

with

$$W^* = \arg\min_{W\in R^l}\left\{\sup_{Z\in\Omega_Z}|f(Z) - W^T\Phi(Z)|\right\} \tag{8}$$

being the ideal weight vector and $|\delta(Z)| < \varepsilon$ ($\varepsilon > 0$) being the approximation error.

3 Control design

In this section, we first introduce a novel compensation mechanism. Then, based on the compensation mechanism, we will focus on the system (1) to design the disturbance-observer-based adaptive tracking controller by using the idea of backstepping technique and the DSC technique.

3.1 Compensation design

Firstly, we present the following auxiliary system to compensate the effect caused by input delay and dead-zone

$$\begin{cases} \dot{\mu}_1 = \mu_2 - h_1\mu_1 \\ \dot{\mu}_i = \mu_{i+1} - h_i\mu_i - g_{i-1}\mu_{i-1}, \quad i = 2,3,\cdots,n-1 \\ \dot{\mu}_n = -h_n\mu_n - g_{n-1}\mu_{n-1} + D(v(t-\tau)) - D(v(t)) \end{cases} \tag{9}$$

where $h_1 - \frac{|1-g_1|}{2} > 0$, $h_i - \frac{|1-g_i|+|1-g_{i-1}|}{2} > 0$, $i = 2,3,\cdots,n-1$ and $h_n - \frac{|1-g_{n-1}|}{2} - 1 > 0$.

Remark 3 It should be noted that, if input delay $\tau = 0$, then $\mu_i (i = 1,2,\cdots,n)$ in (9) are zero when $\mu_i(0) = 0$.

Next, the following change of coordinate is employed in the process of backstepping designing

$$\begin{aligned} z_1 &= x_1 - y_d - \mu_1 \\ z_i &= x_i - \omega_i - \mu_i, \quad i = 2,3,\cdots,n \end{aligned} \tag{10}$$

where ω_i is the first-order filter output signal, which is defined as

$$\xi_i\dot{\omega}_i + \omega_i = \alpha_{i-1}, \omega_i(0) = \alpha_{i-1}(0) \tag{11}$$

with ξ_i being design parameter and α_i being the first-order filter input signals. The filter errors are given by

$$e_i = \omega_i - \alpha_{i-1} \quad i = 2,3,\cdots,n \tag{12}$$

Remark 4 In (10), the change of coordinate is a compensation mechanism, when the system has input delay the auxiliary signal μ_i will be utilized to compensate the effect caused by time delay at the last step.

3.2 Controller design

According to the previous compensation design, the specific design steps of the controller are described as follows.

Step 1: Based on (1) and (9), the time derivative of z_1 can be obtained that

$$\begin{aligned} \dot{z}_1 &= \dot{x}_1 - \dot{\mu}_1 - \dot{y}_d \\ &= f_1(\bar{x}) + x_2 + d_1 - \mu_2 + h_1\mu_1 - \dot{y}_d \end{aligned} \tag{13}$$

Let x_2 be a desired virtual input, then we design the desired feedback signal α_1^* as

$$\alpha_1^* = -k_1 z_1 - f_1(\bar{x}) - d_1 - h_1\mu_1 + \dot{y}_d \tag{14}$$

Based on the idea of approximation by NNS, for given $\varepsilon_1 > 0$, a suitable neural network $W_1^{*T}\Phi_1(Z_1)$ can be selected to approximate the function $f_1(\bar{x})$, which satisfies that

$$f_1(\bar{x}) = W_1^{*T}\Phi_1(Z_1) + \delta_1(Z_1), \quad |\delta_1(Z_1)| \le \varepsilon_1 \tag{15}$$

where $Z_1 = [x_1]^T$ and $\delta_1(Z_1)$ denote the input vector and the approximation error, respectively.

Then (14) can be rewritten as

$$\alpha_1^* = -k_1 z_1 - W_1^{*T}\Phi_1(Z_1) - D_1 - h_1\mu_1 + \dot{y}_d \tag{16}$$

where $D_1 = \delta_1(Z_1) + d_1 \le \varepsilon_1 + d_{1U} = \bar{D}_1$. In addition, based on Assumption 4 and the idea of NNS approximation, $\dot{D}_1$ is bounded, i.e., $|\dot{D}_1| \le \bar{\dot{D}}_1$.

Owing to W_1^* and D_1 are unknown, thus $\hat{W}_1$ and $\hat{D}_1$ are used to estimate W_1^* and D_1, respectively. Then we design the virtual control law and the adaptive law as

$$\alpha_1 = -k_1 z_1 - \hat{W}_1^T\Phi_1(Z_1) - \hat{D}_1 - h_1\mu_1 + \dot{y}_d \tag{17}$$

$$\dot{\hat{W}}_1 = \Lambda_1 z_1\Phi_1(Z_1) - \sigma_1\hat{W}_1 \tag{18}$$

where $\Lambda_1 = \Lambda_1^T > 0$ and $\sigma_1 > 0$ are the design parameters.

To deal with the problem of "explosion of complexity" caused by repeatedly differentiating α_1, let α_1 pass through a given low-pass filter ω_2, which defined in (11) with the filter time design parameter ξ_2 and the filter error e_2 defined in (12). Then one can get

$$\dot{\omega}_2 = \frac{-e_2}{\xi_2} \tag{19}$$

and

$$\dot{e}_2 = \dot{\omega}_2 - \dot{\alpha}_1 = \frac{-e_2}{\xi_2} - \dot{\alpha}_1 = \frac{-e_2}{\xi_2} + M_2(\cdot) \tag{20}$$

where $M_2(\cdot)$ is a continuous function, and $M_2(z_1, z_2, e_2, \hat{W}_1, y_d, \dot{y}_d, \ddot{y}_d, \hat{D}_1, \mu_1) = -(\frac{\partial \alpha_1}{\partial x_1}\dot{x}_1 + \frac{\partial \alpha_1}{\partial z_1}\dot{z}_1 + \frac{\partial \alpha_1}{\partial \hat{W}_1}\dot{\hat{W}}_1 + \frac{\partial \alpha_1}{\partial y_d}\dot{y}_d + \frac{\partial \alpha_1}{\partial \hat{D}_1}\dot{\hat{D}}_1 + \frac{\partial \alpha_1}{\partial \mu_1}\dot{\mu}_1)$. Furthermore, for any given B_0 and ϑ, the sets $\Theta_0 := \{(y_d, \dot{y}_d, \ddot{y}_d) : (y_d)^2 + (\dot{y}_d)^2 + (\ddot{y}_d)^2 \le B_0\}$ is compact in R^3, and $\Theta_2 := \{\sum_{j=1}^{2} z_j^2 + \tilde{W}_1^T \Lambda^{-1} \tilde{W}_1 + e_2^2 \le 2\vartheta\}$ is compact in R^{N_1+3} with N_1 being the dimension of $\tilde{W}_1^T$. According [57], M_2 has a maximum value B_2.

Based on (10), (12) and (17), we can have

$$\begin{aligned} \dot{z}_1 &= W_1^{*T}\Phi_1(Z_1) + z_2 + \alpha_1 + e_2 + D_1 + h_1\mu_1 - \dot{y}_d \\ &= -k_1 z_1 + \tilde{W}_1^T \Phi_1(Z_1) + \tilde{D}_1 + z_2 + e_2 \end{aligned} \tag{21}$$

where $\tilde{W}_1 = W_1^* - \hat{W}_1$ and $\tilde{D}_1 = D_1 - \hat{D}_1$ represent the estimation errors for W_1^* and D_1, respectively.

Furthermore, in order to estimate D_1, an auxiliary variable γ_1 is introduced to design a DO, i.e.,

$$\gamma_1 = z_1 - o_1 \tag{22}$$

with o_1 being an intermedial variable defined as

$$\dot{o}_1 = p_1\gamma_1 + x_2 - \dot{y}_d - \mu_2 + h_1\mu_1 \tag{23}$$

where $p_1 > 0$ is a designed parameter.

According (21), (22) and (23), differentiating γ_1, then

$$\dot{\gamma}_1 = \dot{z}_1 - \dot{o}_1 = W_1^{*T}\Phi_1(Z_1) + D_1 - p_1\gamma_1 \tag{24}$$

Defining the DO as

$$\dot{\hat{D}}_1 = l_1(\gamma_1 - \varphi_1) \tag{25}$$

with $l_1 > 0$ being a design parameter, φ_1 being an intermedial variable defined as

$$\dot{\varphi}_1 = -p_1\gamma_1 + \hat{D}_1 \tag{26}$$

Based on (24) and (26), differentiating $\hat{D}_1$, then

$$\dot{\hat{D}}_1 = l_1 W_1^{*T}\Phi_1(Z_1) + l_1\tilde{D}_1 \tag{27}$$

Furthermore, one can get

$$\dot{\tilde{D}}_1 = \dot{D}_1 - l_1 W_1^{*T}\Phi_1(Z_1) - l_1\tilde{D}_1 \tag{28}$$

From (24), (28) and (20), according to Young's inequality and Assumption 4, one can get the following inequalities (29), (30) and (31) .

$$\begin{aligned} \gamma_1\dot{\gamma}_1 &= \gamma_1 W_1^{*T}\Phi_1(Z_1) + \gamma_1 D_1 - p_1\gamma_1^2 \\ &\le r_1\phi_1^2\gamma_1^2 + \frac{1}{r_1}||W_1^{*T}||^2 + \frac{1}{2}\gamma_1^2 + \frac{1}{2}D_1^2 - p_1\gamma_1^2 \\ &\le -(p_1 - r_1\phi_1^2 - \frac{1}{2})\gamma_1^2 + \frac{1}{r_1}||W_1^{*T}||^2 + \frac{1}{2}\bar{D}_1^2 \end{aligned} \tag{29}$$

$$\begin{aligned} \tilde{D}_1\dot{\tilde{D}}_1 &= \tilde{D}_1\dot{D}_1 - l_1\tilde{D}_1 W_1^{*T}\Phi_1(Z_1) - l_1\tilde{D}_1\tilde{D}_1 \\ &\le \frac{1}{2}\tilde{D}_1^2 + \frac{1}{2}\dot{D}_1^2 + r_1\phi_1^2\tilde{D}_1^2 + \frac{l_1^2}{r_1}||W_1^{*T}||^2 - l_1\tilde{D}_1^2 \\ &\le -(-\frac{1}{2} - r_1\phi_1^2 + l_1)\tilde{D}_1^2 + \frac{1}{2}\bar{D}_1^2 + \frac{l_1^2}{r_1}||W_1^{*T}||^2 \end{aligned} \tag{30}$$

where $|\Phi_1(Z_1)| \le \phi_1$, $r_1 > 0$ is a design parameter.

$$\begin{aligned} e_2\dot{e}_2 &= e_2(\frac{-e_2}{\xi_2}) + e_2 M_2(z_1, z_2, e_2, \hat{W}_1, y_d, \dot{y}_d, \ddot{y}_d, \hat{D}_1, \mu_1) \\ &\le -\frac{1}{\xi_2}e_2^2 + \frac{1}{2}e_2^2 + \frac{1}{2}B_2^2 \end{aligned} \tag{31}$$

Now, the Lyapunov function is taken as

$$V_1 = \frac{1}{2}z_1^2 + \frac{1}{2}\tilde{W}_1^T\Lambda_1^{-1}\tilde{W}_1 + \frac{1}{2}\gamma_1^2 + \frac{1}{2}\tilde{D}_1^2 + \frac{1}{2}e_2^2 \tag{32}$$

It should be noted that the factor $\frac{1}{2}$ is employed in the Lyapunov function V_1, which is often employed in the backstepping design process. The main reason is that the Lyapunov function takes the form of square, thus the employed factor $\frac{1}{2}$ is convenient for us to carry out the theoretical derivation in the process of backstepping design and stability analysis. In other words, the factor $\frac{1}{2}$ can be chosen the other positive constant, which might cause inconvenience to the design process.

Differentiating V_1, then

$$\begin{aligned} \dot{V}_1 &= z_1(-k_1 z_1 + \tilde{W}_1^T\Phi_1(Z_1) + \tilde{D}_1 + z_2 + e_2) - \tilde{W}_1^T\Lambda_1^{-1}\dot{\hat{W}}_1 \\ &\quad + \gamma_1\dot{\gamma}_1 + \tilde{D}_1\dot{\tilde{D}}_1 + e_2\dot{e}_2 \\ &= -k_1 z_1^2 + z_1 z_2 + z_1 e_2 + z_1\tilde{D}_1 + \sigma_1\tilde{W}_1^T\hat{W}_1 + \gamma_1\dot{\gamma}_1 \\ &\quad + \tilde{D}_1\dot{\tilde{D}}_1 + e_2\dot{e}_2 \end{aligned} \tag{33}$$

Substituting (29), (30) and (31) into (33), and using the complete squares formula, then

$$\begin{aligned}\dot{V}_1 \le & -k_1 z_1^2 + z_1 z_2 + \frac{1}{2} z_1^2 + \frac{1}{2} e_2^2 + \frac{1}{2} z_1^2 + \frac{1}{2} \bar{D}_1^2 \\ & - \sigma_1 \tilde{W}_1^T \hat{W}_1 + \gamma_1 \dot{\gamma}_1 + \tilde{D}_1 \dot{\tilde{D}}_1 + e_2 \dot{e}_2 \\ \le & -(k_1 - 1) z_1^2 - (p_1 - r_1 \phi_1^2 - \frac{1}{2}) \gamma_1^2 \\ & - (-1 - r_1 \phi_1^2 + l_1) \tilde{D}_1^2 \\ & - (\frac{1}{\xi_2} - 1) e_2^2 \\ & + z_1 z_2 + \sigma_1 \tilde{W}_1^T \hat{W}_1 + \frac{l_1^2 + 1}{r_1} ||W_1^{*T}||^2 \\ & + \frac{1}{2} \bar{D}_1^2 + \frac{1}{2} \bar{D}_1^2 + \frac{1}{2} B_2^2 \end{aligned} \tag{34}$$

Step i ($2 \le i \le n-1$): Based on (1) and (9), differentiating $z_i = x_i - \omega_i - \mu_i$, then

$$\dot{z}_i = f_i(\bar{x}) + x_{i+1} + d_i - \dot{\omega}_i - \mu_{i+1} + h_i \mu_i + g_{i-1} \mu_{i-1} \tag{35}$$

Let x_{i+1} be a desired virtual input, we define the desired feedback signal α_i^* as

$$\alpha_i^* = -z_{i-1} - k_i z_i - f_i(\bar{x}) - d_i - h_i \mu_i - g_{i-1} \mu_{i-1} + \dot{\omega}_i \tag{36}$$

As the first step, based on the idea of approximation, the nonlinear function $f_i(\bar{x})$ can be approximated by $W_i^{*T} \Phi_i(Z_i)$, which yields

$$f_i(\bar{x}) = W_i^{*T} \Phi_i(Z_i) + \delta_i(Z_i), \quad |\delta_i(Z_i)| \le \varepsilon_i \tag{37}$$

where $\delta_i(Z_i)$ and $Z_i = [x_1, x_2, \cdots, x_i]^T$ denote the approximation error and input vector, respectively.

Substituting (37) into (36), then α_i^* can be rewritten as

$$\alpha_i^* = -z_{i-1} - k_i z_i - W_i^{*T} \Phi_i(Z_i) - D_i - h_i \mu_i - g_{i-1} \mu_{i-1} + \dot{\omega}_i \tag{38}$$

where $D_i = \delta_i(Z_i) + d_i \le \varepsilon_i + d_{iU} = \bar{D}_i$. Based on Assumption 4 and the idea of NNS approximation, $\dot{D}_i$ is bounded, i.e., $|\dot{D}_i| \le \bar{\dot{D}}_i$.

Because W_i^* and D_i are unknown, thus we use $\hat{W}_i$ and $\hat{D}_i$ to estimate W_i^* and D_i, respectively. Then, we design the virtual control law and the adaptive law as

$$\alpha_i = -z_{i-1} - k_i z_i - \hat{W}_i^T \Phi_i(Z_i) - \hat{D}_i - h_i \mu_i - g_{i-1} \mu_{i-1} + \dot{\omega}_i \tag{39}$$

$$\dot{\hat{W}}_i = \Lambda_i z_i \Phi_i(Z_i) - \sigma_i \hat{W}_i \tag{40}$$

with $\Lambda_i = \Lambda_i^T > 0$ and $\sigma_i > 0$ being the design parameters.

To deal with the "explosion of complexity" problem caused by repeatedly differentiating α_i, let α_i pass through the low-pass filter ω_{i+1} defined in (11) with the filter time design parameter ξ_{i+1} and the filter error e_{i+1} defined in (12). Thus, one can have

$$\dot{\omega}_{i+1} = \frac{-e_{i+1}}{\xi_{i+1}} \tag{41}$$

and

$$\dot{e}_{i+1} = \dot{\omega}_{i+1} - \dot{\alpha}_i = \frac{-e_{i+1}}{\xi_{i+1}} - \dot{\alpha}_i = \frac{-e_{i+1}}{\xi_{i+1}} + M_{i+1}(\cdot) \tag{42}$$

where $M_{i+1}(\cdot)$ is a continuous function, and $M_{i+1}(\cdot) = M_{i+1}(z_1, \cdots, z_{i+1}, e_2, \cdots, e_{i+1}, \hat{W}_1, \cdots, \hat{W}_i, y_d, \dot{y}_d, \ddot{y}_d, \hat{D}_1, \cdots, \hat{D}_i, \mu_1, \cdots, \mu_i) = -(\frac{\partial \alpha_i}{\partial x_i} \dot{x}_i + \frac{\partial \alpha_i}{\partial z_i} \dot{z}_i + \frac{\partial \alpha_i}{\partial \hat{W}_i} \dot{\hat{W}}_i + \frac{\partial \alpha_i}{\partial y_d} \dot{y}_d + \frac{\partial \alpha_i}{\partial \hat{D}_i} \dot{\hat{D}}_i + \frac{\partial \alpha_i}{\partial \mu_i} \dot{\mu}_i)$. For any given B_0 and ϑ, the sets $\Theta_0 := \{(y_d, \dot{y}_d, \ddot{y}_d) : (y_d)^2 + (\dot{y}_d)^2 + (\ddot{y}_d)^2 \le B_0\}$ is compact in R^3 and $\Theta_i := \{\sum_{j=1}^{i} z_j^2 + \tilde{W}_1^T \Lambda^{-1} \tilde{W}_1 + e_{i+1}^2 \le 2\vartheta\}$ is in $R^{\sum_{j=1}^{i} N_i + 2i - 1}$ with N_i being the dimension of $\tilde{W}_i^T$. According [57], M_{i+1} has a maximum value B_{i+1}.

With the aid of $x_{i+1} = z_{i+1} + \alpha_i + e_{i+1} + \mu_{i+1}$ and based on (39), then (35) can be rewritten as

$$\dot{z}_i = -z_{i-1} - k_i z_i + \tilde{W}_i^T \Phi_i(Z_i) + \tilde{D}_i + z_{i+1} + e_{i+1} \tag{43}$$

where $\tilde{W}_i = W_i^* - \hat{W}_i$ and $\tilde{D}_i = D_i^* - \hat{D}_i$ represent the estimation errors for W_i^* and D_i, respectively.

In what follows, to estimate D_i, an auxiliary variable γ_i is introduced to design a DO, i.e.,

$$\gamma_i = z_i - o_i \tag{44}$$

with o_i being an intermedial variable defined as

$$\dot{o}_i = p_i \gamma_i + x_{i+1} - \dot{\omega}_i - \mu_{i+1} + h_i \mu_i + g_{i-1} \mu_{i-1} \tag{45}$$

where $p_i > 0$ is a designed parameter.

Based on (43), (44) and (45), differentiating γ_i, then

$$\dot{\gamma}_i = W_i^{*T} \Phi_i(Z_i) + D_i - p_i \gamma_i \tag{46}$$

Let the DO be designed as

$$\dot{\hat{D}}_i = l_i(\gamma_i - \varphi_i) \tag{47}$$

with $l_i > 0$ being a design parameter, φ_i being an intermedial variable defined as

$$\dot{\varphi}_i = -p_i \gamma_i + \hat{D}_i \tag{48}$$

According (46) and (48), differentiating $\hat{D}_i$, then

$$\dot{\hat{D}}_i = l_i W_i^{*T} \Phi_i(Z_i) + l_i \tilde{D}_i \tag{49}$$

Furthermore, one can get

$$\dot{\tilde{D}}_i = \dot{D}_i - l_i W_i^{*T} \Phi_i(Z_i) - l_i \tilde{D}_i \tag{50}$$

Based on (46), (50) and (42), according to Young's

inequality and Assumption 4, one can get the following inequalities (51), (52) and (53).

$$\begin{aligned}\gamma_i\dot{\gamma}_i &= \gamma_i W_i^{*T}\Phi_i(Z_i) + \gamma_i D_i - p_i\gamma_i^2 \\ &\le r_i\phi_i^2\gamma_i^2 + \frac{1}{r_i}||W_i^{*T}||^2 + \frac{1}{2}\gamma_i^2 + \frac{1}{2}D_i^2 - p_i\gamma_i^2 \\ &\le -(p_i - r_i\phi_i^2 - \frac{1}{2})\gamma_i^2 + \frac{1}{r_i}||W_i^{*T}||^2 + \frac{1}{2}\bar{D}_i^2\end{aligned} \tag{51}$$

$$\begin{aligned}\tilde{D}_i\dot{\tilde{D}}_i &= \tilde{D}_i\dot{D}_i - l_i\tilde{D}_i W_i^{*T}\Phi_i(Z_i) - l_i\tilde{D}_i\tilde{D}_i \\ &\le \frac{1}{2}\hat{D}_i^2 + \frac{1}{2}\dot{D}_i^2 + r_i\phi_i^2\tilde{D}_i^2 + \frac{l_i^2}{r_i}||W_i^{*T}||^2 - l_i\tilde{D}_i^2 \\ &\le -(-\frac{1}{2} - r_i\phi_i^2 + l_i)\tilde{D}_i^2 + \frac{1}{2}\bar{\dot{D}}_i^2 + \frac{l_i^2}{r_i}||W_i^{*T}||^2\end{aligned} \tag{52}$$

where $|\Phi_i(Z_i)| \le \phi_i$, $r_i > 0$ is a design parameter.

$$\begin{aligned}e_{i+1}\dot{e}_{i+1} &= e_{i+1}(\frac{-e_{i+1}}{\xi_{i+1}}) + e_{i+1}M_{i+1}(\cdot) \\ &\le -\frac{1}{\xi_{i+1}}e_{i+1}^2 + \frac{1}{2}e_{i+1}^2 + \frac{1}{2}B_{i+1}^2\end{aligned} \tag{53}$$

Considering the Lyapunov function candidate be

$$V_i = \frac{1}{2}z_i^2 + \frac{1}{2}\tilde{W}_i^T\Lambda_i^{-1}\tilde{W}_i + \frac{1}{2}\gamma_i^2 + \frac{1}{2}\tilde{D}_i^2 + \frac{1}{2}e_{i+1}^2 \tag{54}$$

Differentiating V_i

$$\begin{aligned}\dot{V}_i &= -z_{i-1}z_i - k_i z_i^2 + z_i z_{i+1} + z_i e_{i+1} + z_i\tilde{D}_i \\ &\quad + \sigma_i\tilde{W}_i^T\hat{W}_i + \gamma_i\dot{\gamma}_i + \tilde{D}_i\dot{\tilde{D}}_i + e_{i+1}\dot{e}_{i+1}\end{aligned} \tag{55}$$

Now, substituting (51), (52) and (53) into (55), one can get

$$\begin{aligned}\dot{V}_i &\le -z_{i-1}z_i - k_i z_i^2 + z_i z_{i+1} + z_i^2 + \frac{1}{2}e_{i+1}^2 + \frac{1}{2}\tilde{D}_i^2 + \sigma_i\tilde{W}_i^T\hat{W}_i \\ &\quad + \gamma_i\dot{\gamma}_i + \tilde{D}_i\dot{\tilde{D}}_i + e_{i+1}\dot{e}_{i+1} \\ &\le -(k_i - 1)z_i^2 - (p_i - r_i\phi_i^2 - \frac{1}{2})\gamma_i^2 - (-1 - r_i\phi_i^2 + l_i)\tilde{D}_i^2 \\ &\quad - (\frac{1}{\xi_{i+1}} - 1)e_{i+1}^2 - z_{i-1}z_i + z_i z_{i+1} + \sigma_i\tilde{W}_i^T\hat{W}_i \\ &\quad + \frac{l_i^2 + 1}{r_i}||W_i^{*T}||^2 \\ &\quad + \frac{1}{2}\bar{D}_i^2 + \frac{1}{2}\bar{\dot{D}}_i^2 + \frac{1}{2}B_{i+1}^2\end{aligned} \tag{56}$$

Step n: According (1) and (9), the time derivative of z_n as

$$\begin{aligned}\dot{z}_n &= \dot{x}_n - \dot{\omega}_n - \dot{\mu}_n \\ &= f_n(\bar{x}) + d_n - \dot{\omega}_n + h_n\mu_n + g_{n-1}\mu_{n-1} + mv(t) + d(v(t))\end{aligned} \tag{57}$$

As in step i, for given $\varepsilon_n > 0$, $f_n(\bar{x})$ can be modeled by a suitable $W_n^{*T}\Phi_n(Z_n)$, i.e.,

$$f_n(\bar{x}) = W_n^{*T}\Phi_n(Z_n) + \delta_n(Z_n), \quad |\delta_n(Z_n)| \le \varepsilon_n \tag{58}$$

where $\delta_n(Z_n)$ and $Z_n = [x_1, x_2, \cdots, x_n]^T$ denote the approximation error and input vector, respectively.

Substituting (58) into (57), then (57) can be rewritten as

$$\begin{aligned}\dot{z}_n &= W_n^{*T}\Phi_n(Z_n) + \delta_n(Z_n) + d_n - \dot{\omega}_n \\ &\quad + h_n\mu_n + g_{n-1}\mu_{n-1} + mv(t) + d(v(t))\end{aligned} \tag{59}$$

Now, design the desired feedback control v^* as

$$\begin{aligned}v^* &= \frac{1}{m}(-z_{n-1} - k_n z_n - W_n^{*T}\Phi_n(Z_n) \\ &\quad - D_n - h_n\mu_n - g_{n-1}\mu_{n-1} + \dot{\omega}_n)\end{aligned} \tag{60}$$

where $D_n = \delta_n(Z_n) + d_n + d(v(t))$. By using Assumption 4, the idea of NNS approximation, and taking $|d(v(t))| \le d^*$ into account, one can get $D_n \le \varepsilon_n + d_{nU} + d^* = \bar{D}_n$ and $|\dot{D}_n|$ is bounded, i.e., $|\dot{D}_n| \le \bar{\dot{D}}_n$.

Since W_n^* and D_n are unknown, we use $\hat{W}_n$ and $\hat{D}_n$ to estimate W_n^* and D_n, respectively. Then, the desired feedback control is designed as

$$\begin{aligned}v &= \frac{1}{m}(-z_{n-1} - k_n z_n - \hat{W}_n{}^T\Phi_n(Z_n) \\ &\quad - \hat{D}_n - h_n\mu_n - g_{n-1}\mu_{n-1} + \dot{\omega}_n)\end{aligned} \tag{61}$$

and the adaptive law is designed as

$$\dot{\hat{W}}_n = \Lambda_n z_n\Phi_n(Z_n) - \sigma_n\hat{W}_n \tag{62}$$

where $\Lambda_n = \Lambda_n^T > 0$ and $\sigma_n > 0$ the design parameters.

Substituting (61) into (59), one can get

$$\dot{z}_n = -z_{n-1} - k_n z_n + \tilde{W}_n^T\Phi_n(Z_n) + \tilde{D}_n \tag{63}$$

where $\tilde{W}_n = W_n^* - \hat{W}_n$ and $\tilde{D}_n = D_n^* - \hat{D}_n$ represent the estimation errors for W_n^* and D_n, respectively.

Next, to estimate D_n, an auxiliary variable γ_n is proposed to design a DO, i.e.,

$$\gamma_n = z_n - o_n \tag{64}$$

with o_n being an intermedial variable defined as

$$\dot{o}_n = p_n\gamma_n + mv - \dot{\omega}_n + h_n\mu_n + g_{n-1}\mu_{n-1} \tag{65}$$

where $p_n > 0$ is a designed parameter.

Based on (63), (64) and (65), differentiating γ_n, then

$$\dot{\gamma}_n = W_n^{*T}\Phi_n(Z_n) + D_n - p_n\gamma_n \tag{66}$$

Let the DO be designed as

$$\hat{D}_n = l_n(\gamma_n - \varphi_n) \tag{67}$$

with $l_n > 0$ being a design parameter, φ_n being an intermedial variable defined as

$$\dot{\varphi}_n = -p_n\gamma_n + \hat{D}_n \tag{68}$$

Based on (66) and (68), differentiating $\hat{D}_n$, then

$$\dot{\hat{D}}_n = l_n W_n^{*T}\Phi_n(Z_n) + l_n\tilde{D}_n \tag{69}$$

Furthermore, one can get

$$\dot{\tilde{D}}_n = \dot{D}_n - l_n W_n^{*T}\Phi_n(Z_n) - l_n\tilde{D}_n \tag{70}$$

Similar to Step i, according to (66) and (69) and according to Young's inequality and Assumption 4, one can get the following inequalities (71) and (72).

$$\begin{aligned}\gamma_n\dot{\gamma}_n &= \gamma_n W_n^{*T}\Phi_n(Z_n) + \gamma_n D_n - p_n\gamma_n^2\\ &\le r_n\phi_n^2\gamma_n^2 + \frac{1}{r_n}||W_n^{*T}||^2 + \frac{1}{2}\gamma_n^2 + \frac{1}{2}D_n^2 - p_n\gamma_n^2\\ &\le -(p_n - r_n\phi_n^2 - \frac{1}{2})\gamma_n^2 + \frac{1}{r_n}||W_n^{*T}||^2 + \frac{1}{2}\bar{D}_n^2\end{aligned} \tag{71}$$

$$\begin{aligned}\tilde{D}_n\dot{\tilde{D}}_n &= \tilde{D}_n\dot{D}_n - l_n\tilde{D}_n W_n^{*T}\Phi_n(Z_n) - l_n\tilde{D}_n\tilde{D}_n\\ &\le \frac{1}{2}\tilde{D}_n^2 + \frac{1}{2}\dot{D}_n^2 + r_n\phi_n^2\tilde{D}_n^2 + \frac{l_n^2}{r_n}||W_n^{*T}||^2 - l_n\tilde{D}_n^2\\ &\le -(-\frac{1}{2} - r_n\phi_n^2 + l_n)\tilde{D}_n^2 + \frac{1}{2}\bar{\dot{D}}_n^2 + \frac{l_n^2}{r_n}||W_n^{*T}||^2\end{aligned} \tag{72}$$

where $|\Phi_n(Z_n)| \le \phi_n$, $r_n > 0$ is a design parameter.

Then, the Lyapunov function is taken as

$$V_n = \frac{1}{2}z_n^2 + \frac{1}{2}\tilde{W}_n^T\Lambda_n^{-1}\tilde{W}_n + \frac{1}{2}\gamma_n^2 + \frac{1}{2}\tilde{D}_n^2 \tag{73}$$

Differentiating V_n

$$\begin{aligned}\dot{V}_n &= z_n(-z_{n-1} - k_n z_n + \tilde{W}_n^T\Phi_n(Z_n) + \tilde{D}_n)\\ &\quad - \tilde{W}_n^T\Lambda_n^{-1}\dot{\hat{W}}_n + \gamma_n\dot{\gamma}_n + \tilde{D}_n\dot{\tilde{D}}_n\\ &= -z_{n-1}z_n - k_n z_n^2 + z_n\tilde{D}_n + \sigma_n\tilde{W}_n^T\hat{W}_n + \gamma_n\dot{\gamma}_n + \tilde{D}_n\dot{\tilde{D}}_n\end{aligned} \tag{74}$$

Consequently, substituting (63), (71) and (72) into (74), we can have the following result

$$\begin{aligned}\dot{V}_n &\le -z_{n-1}z_n - k_n z_n^2 + z_n^2 + \frac{1}{2}\tilde{D}_n^2 + \sigma_n\tilde{W}_n^T\hat{W}_n + \gamma_n\dot{\gamma}_n + \tilde{D}_n\dot{\tilde{D}}_n\\ &\le -(k_n - 1)z_n^2 - (p_n - r_n\phi_n^2 - \frac{1}{2})\gamma_n^2\\ &\quad - (-1 - r_n\phi_n^2 + l_n)\tilde{D}_n^2\\ &\quad - z_{n-1}z_n + \sigma_n\tilde{W}_n^T\hat{W}_n + \frac{l_n^2+1}{r_n}||W_n^{*T}||^2\\ &\quad + \frac{1}{2}\tilde{D}_n^2 + \frac{1}{2}\bar{D}_n^2\end{aligned} \tag{75}$$

3.3 Main result

Based on the above detailed design procedures, now the main result can be described by the following theorem.

Theorem 1 *Based on Assumptions 1–5, for system (1) the disturbance observer is designed in (25), (47), (67), the virtual signals defined in (17), (39) for $1 \le i \le n-1$, the real controller defined in (61), and the adaptive law defined in (40) for $1 \le i \le n$, which can ensure that all the signals of the closed-loop system are bounded, and the tracking error converges to a bounded compact set near the origin.*

Proof Firstly, we design the following Lyapunov function candidate to discuss the stability of the closed-loop system.

$$\begin{aligned}V &= \sum_{i=1}^{n} V_n = \sum_{i=1}^{n}\left(\frac{1}{2}z_i^2 + \frac{1}{2}\tilde{W}_i^T\Lambda_i^{-1}\tilde{W}_i + \frac{1}{2}\gamma_i^2 + \frac{1}{2}\tilde{D}_i^2\right)\\ &\quad + \sum_{i=1}^{n-1}\left(\frac{1}{2}e_{i+1}^2\right)\end{aligned} \tag{76}$$

Based on the fact $\tilde{W}_i^T\hat{W}_i \le \frac{1}{2}||W_i^*||^2 - \frac{1}{2}||\tilde{W}_i||^2$ for $i = 1, \cdots, n$, and differentiating V_n, then

$$\begin{aligned}\dot{V} &\le -\sum_{i=1}^{n}(k_i - 1)z_i^2 + \sum_{i=1}^{n}\sigma_i\tilde{W}_i^T\hat{W}_i - \sum_{i=1}^{n}(p_i - r_i\phi_i^2 - \frac{1}{2})\gamma_i^2\\ &\quad - \sum_{i=1}^{n}(-1 - r_i\phi_i^2 + l_i)\tilde{D}_i^2 - \sum_{i=1}^{n-1}(\frac{1}{\xi_{i+1}} - 1)e_{i+1}^2\\ &\quad + \sum_{i=1}^{n}\left(\frac{l_i^2+1}{r_i}||W_i^{*T}||^2 + \frac{1}{2}\bar{D}_i^2 + \frac{1}{2}\bar{\dot{D}}_i^2\right) + \sum_{i=1}^{n-1}\frac{1}{2}B_{i+1}^2\\ &\le -\sum_{i=1}^{n}(k_i - 1)z_i^2 - \sum_{i=1}^{n}\frac{\sigma_i}{2}||\tilde{W}_i||^2 - \sum_{i=1}^{n}(p_i - r_i\phi_i^2 - \frac{1}{2})\gamma_i^2\\ &\quad - \sum_{i=1}^{n}(-1 - r_i\phi_i^2 + l_i)\tilde{D}_i^2 - \sum_{i=1}^{n-1}(\frac{1}{\xi_{i+1}} - 1)e_{i+1}^2\\ &\quad + \sum_{i=1}^{n}\left(\left(\frac{\sigma_i}{2} + \frac{l_i^2+1}{r_i}\right)||W_i^{*T}||^2 + \frac{1}{2}\bar{D}_i^2 + \frac{1}{2}\bar{\dot{D}}_i^2\right)\\ &\quad + \sum_{i=1}^{n-1}\frac{1}{2}B_{i+1}^2\\ &= -cV + d\end{aligned} \tag{77}$$

where $c = \min\{2(k_i - 1) : 1 \le i \le n, \frac{\sigma_i}{\lambda_{\max}(\Lambda_i^{-1})} : 1 \le i \le n, 2(p_i - r_i\phi_i^2 - \frac{1}{2}) : 1 \le i \le n, 2(-1 - r_i\phi_i^2 + l_i) : 1 \le i \le n, (\frac{1}{\xi_{i+1}} - 1) : 1 \le i \le n-1\}$, and

$$d = \sum_{i=1}^{n}\left(\left(\frac{\sigma_i}{2}+\frac{l_i^2+1}{r_i}\right)||W_i^{*T}||^2+\frac{1}{2}\bar{D}_i^2+\frac{1}{2}\bar{\bar{D}}_i^2\right) + \sum_{i=1}^{n-1}\frac{1}{2}B_{i+1}^2$$

Multiplying (77) by e^{ct} on both sides, and integrating from 0 to t, one can get

$$V(t) \le \left(V(0)-\frac{d}{c}\right)e^{-ct}+\frac{d}{c} \tag{78}$$

For (78), if $t \to \infty$, then $e^{-ct} \to 0$ and V is convergent. This means that all the signals z_i, $\tilde{W}_i$, γ_i, $\tilde{D}_i$ and e_{i+1} are all bounded.

In what follows, we consider the boundedness of μ_i. Let the Lyapunov function defined as

$$V_{\mu_0} = \frac{1}{2}\sum_{i=1}^{n}\mu_i^2+\frac{1}{\beta}\int_{t-\tau}^{t}\int_{\theta}^{t}||\dot{v}(s)||^2 ds d\theta \tag{79}$$

Thus, the derivative of V_{μ_0} satisfies that

$$\begin{aligned}
\dot{V}_{\mu_0} &\le \mu_1(\mu_2-p_1\mu_1)+\sum_{i=2}^{n-1}\mu_i(\mu_{i+1}-p_i\mu_i-g_{i-1}\mu_{i-1}) \\
&\quad+\mu_n(-p_n\mu_n-g_{n-1}\mu_{n-1}+D(v(t-\tau))-D(v(t))) \\
&\quad+\frac{\tau}{\beta}||\dot{v}(t)||^2-\frac{1}{\beta}\int_{t-\tau}^{t}||\dot{v}(s)||^2 ds \\
&= \sum_{i=1}^{n-1}((1-g_i)\mu_i\mu_{i+1})+\sum_{i=1}^{n}(-p_i\mu_i^2)+(D(v(t-\tau))-D(v(t)))\mu_n \\
&\quad+\frac{\tau}{\beta}||\dot{v}(t)||^2-\frac{1}{\beta}\int_{t-\tau}^{t}||\dot{v}(s)||^2 ds \\
&\le \sum_{i=1}^{n-1}\frac{|1-g_i|}{2}(\mu_i^2+\mu_{i+1}^2) \\
&\quad+\sum_{i=1}^{n-1}(-p_i\mu_i^2)+(-p_n\mu_n^2)+(mv(t-\tau) \\
&\quad-mv(t))\mu_n+(dv(t-\tau)-dv(t))\mu_n+\frac{\tau}{\beta}||\dot{v}(t)||^2 \\
&\quad-\frac{1}{\beta}\int_{t-\tau}^{t}||\dot{v}(s)||^2 ds \\
&\le -(p_1-\frac{|1-g_1|}{2})\mu_1^2 \\
&\quad-\sum_{i=2}^{n-1}(p_i-\frac{|1-g_{i-1}|}{2}-\frac{|1-g_i|}{2})\mu_i^2-(p_n \\
&\quad-\frac{|1-g_{n-1}|}{2}-1)\mu_n^2+\frac{m^2}{2}||v(t-\tau)-v(t)||^2 \\
&\quad+\frac{1}{2}||dv(t-\tau)-dv(t)||^2 \\
&\quad+\frac{\tau}{\beta}||\dot{v}(t)||^2-\frac{1}{\beta}\int_{t-\tau}^{t}||\dot{v}(s)||^2 ds
\end{aligned} \tag{80}$$

Based on Assumption 3, we have

$$\frac{1}{2}||dv(t-\tau)-dv(t)||^2 \le \frac{1}{2}(||dv(t-\tau)||^2+||dv(t)||^2) \le d^{*2} \tag{81}$$

According to the Cauchy–Schwarz inequality, then

$$\frac{1}{2}||v(t-\tau)-v(t)||^2 \le \frac{\tau}{2}\int_{t-\tau}^{t}||\dot{v}(s)||^2 ds \tag{82}$$

Furthermore, substituting (81) and (82) into (80), one has

$$\begin{aligned}
\dot{V}_{\mu_0} &\le -\sum_{i=1}^{n}\bar{h_i}\mu_i^2-\left(\frac{1}{\beta}-\frac{m\tau}{2}\right)\int_{t-\tau}^{t}||\dot{v}(s)||^2 ds \\
&\quad+\frac{\tau}{\beta}||\dot{v}(t)||^2+d^{*2}
\end{aligned} \tag{83}$$

where $\bar{h_1} = h_1-\frac{|1-g_1|}{2}$, $\bar{h_i} = h_i-\frac{|1-g_i|+|1-g_{i-1}|}{2}$, $i = 2,3,\cdots,n-1$, and $\bar{h_n} = h_n-\frac{|1-g_{n-1}|}{2}-1$.

In what follows, we consider the boundedness of $\frac{\tau}{\beta}||\dot{v}(t)||^2$ in (83).

According to (10), (17), (18), (39),(40),(61) and (62), we describe $v(t)$ and $\dot{v}(t)$ as

$$v(t) = \zeta_1(z_{n-1},z_n,\hat{W}_n,\hat{D}_n)+\zeta_2\mu_n+\zeta_3\mu_{n-1}+\zeta_4(e_n) \tag{84}$$

$$\begin{aligned}
\dot{v}(t) &= \zeta_5(z_{n-2},z_{n-1},z_n,\hat{W}_{n-1},\hat{W}_n,\tilde{D}_n)+\sum_{j=1}^{n}\zeta_{8j}(z,\hat{W})\mu_j \\
&\quad+\zeta_6(M_n(.),e_n)+\zeta_7(z,\hat{W})v(t-\tau)
\end{aligned} \tag{85}$$

where $\zeta_1(.),\zeta_2(.),\cdots,\zeta_7(.)$ and $\zeta_{8j}(.)(1 \le j \le n)$ are C^1 functions. Due to the fact that z_{n-2}, z_{n-1}, z_n, $\hat{W}_{n-1}$, $\hat{W}_n$, $\hat{D}_n$, $\tilde{D}_n$, e_n and $M_n(.)$ are all bounded, therefore, one can obtain that

$$||\zeta_i|| \le \kappa_i, i = 1,2,\cdots,7 \text{ and } ||\zeta_{ik}|| \le \kappa_{jk} \tag{86}$$

where κ_i and $\kappa_{jk}, (j = 8; 1 \le k \le n)$ are the positive constants.

$$\begin{aligned}
||v(t)||^2 &\le (||\zeta_1||+||\zeta_2||\mu_{n-1}+||\zeta_3||\mu_n+||\zeta_4(e_n)||)^2 \\
&\le (\kappa_1+\kappa_2\mu_n+\kappa_3\mu_{n-1}+\kappa_4)^2 \\
&\le 4\kappa_1^2+4\kappa_2^2\mu_n^2+4\kappa_3^2\mu_{n-1}^2+4\kappa_4^2 \\
&\le \kappa_1'+\kappa_2'\mu_n^2+\kappa_3'\mu_{n-1}^2+\kappa_4'
\end{aligned} \tag{87}$$

where $\kappa_1' = 4\kappa_1^2$, $\kappa_2' = 4\kappa_2^2$, $\kappa_3' = 4\kappa_3^2$, and $\kappa_4' = 4\kappa_4^2$. Furthermore, for $v(t-\tau)$ it satisfies that

$$||v(t-\tau)||^2 \le \kappa_1' + \kappa_2'\mu_n^2(t-\tau) + \kappa_3'\mu_{n-1}^2(t-\tau) + \kappa_4' \tag{88}$$

From (85) and (88), the upper boundedness of $\frac{\tau}{\beta}||\dot{v}(t)||^2$ can be estimated by

$$\begin{aligned}
\frac{\tau}{\beta}||\dot{v}(t)||^2 &\le \frac{\tau}{\beta}||\zeta_5 + \sum_{j=1}^{n}\zeta_{8j}(z,\hat{W})\mu_j \\
&\quad + \zeta_6(M_n(.),e_n) + \zeta_7(z,\hat{W})v(t-\tau)||^2 \\
&\le \frac{\tau}{\beta}4(\kappa_5^2 + n\sum_{j=1}^{n}\kappa_{8j}^2\mu_j^2 + \kappa_6^2 + \kappa_7^2 v^2(t-\tau)) \\
&\le \frac{\tau}{\beta}(4\kappa_5^2 + 4\kappa_7^2(\kappa_1' + \kappa_4') + \kappa_6^2 + 4n\sum_{j=1}^{n}\kappa_{8j}^2\mu_j^2 \\
&\quad + 4\kappa_7^2\kappa_2'\mu_n^2(t-\tau) + 4\kappa_7^2\kappa_3'\mu_{n-1}^2(t-\tau)) \\
&\le \frac{\tau}{\beta}(\kappa_5' + \sum_{j=1}^{n}\kappa_{8j}'\mu_j^2 + \kappa_6'\mu_n^2(t-\tau) + \kappa_7'\mu_{n-1}^2(t-\tau))
\end{aligned} \tag{89}$$

where $\kappa_5' = 4\kappa_5^2 + 4\kappa_7^2(\kappa_1' + \kappa_4') + \kappa_6^2$, $\kappa_{8j}' = 4n\kappa_{8j}^2$, $\kappa_6' = 4\kappa_7^2\kappa_2'$ and $\kappa_7' = 4\kappa_7^2\kappa_3'$.

According to (89) and rewriting (83) as

$$\begin{aligned}
\dot{V}_{\mu_0} \le &-\sum_{i=1}^{n}\tilde{h}_i\mu_i^2 - \left(\frac{1}{\beta} - \frac{m\tau}{2}\right)\int_{t-\tau}^{t}||\dot{v}(s)||^2 ds + \frac{\tau\kappa_6'}{\beta}\mu_n^2(t-\tau) \\
&+ \frac{\tau\kappa_7'}{\beta}\mu_{n-1}^2(t-\tau) + d^{*2} + \frac{\tau}{\beta}\kappa_5'
\end{aligned} \tag{90}$$

where $\tilde{h}_i = \bar{h}_i - \frac{\tau}{\beta}\kappa_{8i}'$,$1 \le i \le n$.

For the auxiliary system (9), let the Lyapunov function candidate be

$$\begin{aligned}
V_\mu = V_{\mu 0} &+ \frac{\tau\kappa_6'}{\beta}\int_{t-\tau}^{t}\mu_n^2(s)ds + \frac{1}{\nu_1}\int_{t-\tau}^{t}\int_{\theta}^{t}\mu_n^2(s)dsd\theta \\
&+ \frac{\tau\kappa_7'}{\beta}\int_{t-\tau}^{t}\mu_{n-1}^2(s)ds + \frac{1}{\nu_2}\int_{t-\tau}^{t}\int_{\theta}^{t}\mu_{n-1}^2(s)dsd\theta
\end{aligned} \tag{91}$$

Differentiating V_μ, then

$$\begin{aligned}
\dot{V}_\mu \le &-\sum_{i=1}^{n}\hat{h}_i\mu_i^2 - \left(\frac{1}{\beta} - \frac{m\tau}{2}\right)\int_{t-\tau}^{t}||\dot{v}(s)||^2 ds - \frac{1}{\nu_1}\int_{t-\tau}^{t}\mu_n^2(s)ds \\
&- \frac{1}{\nu_2}\int_{t-\tau}^{t}\mu_{n-1}^2(s)ds + \frac{\tau}{\beta}\kappa_4' + d^{*2} + \frac{\tau}{\beta}\kappa_5'
\end{aligned} \tag{92}$$

where $\hat{h}_i = \tilde{h}_i$ $(1 \le i \le n-2)$, $\hat{h}_{n-1} = \tilde{h}_{n-1} + \frac{\tau}{\beta}\kappa_7' - \frac{\tau}{\nu_2}$, and $\hat{h}_n = \tilde{h}_n + \frac{\tau}{\beta}\kappa_6' - \frac{\tau}{\nu_1}$.

By designing the parameters h_i, β , ν_1 and ν_2, we can have

$$\hat{h}_i > 0,\ \frac{1}{\beta} - \frac{m\tau}{2} > 0 \tag{93}$$

Furthermore, one can get

$$\begin{aligned}
&\int_{t-\tau}^{t}\int_{\theta}^{t}||\dot{v}(s)||^2 dsd\theta \\
&\le \tau\sup_{\theta\in[t-\tau,t]}\int_{t-\tau}^{t}||\dot{v}(s)||^2 ds = \tau\int_{t-\tau}^{t}||\dot{v}(s)||^2 ds
\end{aligned} \tag{94}$$

$$\begin{aligned}
&\int_{t-\tau}^{t}\int_{\theta}^{t}\mu_k^2(s)dsd\theta \\
&\le \tau\sup_{\theta\in[t-\tau,t]}\int_{t-\tau}^{t}\mu_k^2(s)ds = \tau\int_{t-\tau}^{t}\mu_k^2(s)ds, \quad k = n-1, n.
\end{aligned} \tag{95}$$

Consequently, the derivative of V_μ satisfies that

$$\begin{aligned}
\dot{V}_\mu \le &-\sum_{i=1}^{n}\hat{h}_i\mu_i^2 - \left(\frac{1}{\beta} - \frac{m\tau}{2}\right)\int_{t-\tau}^{t}||\dot{v}(s)||^2 ds \\
&- \left(\frac{1}{\nu_1} - \frac{\tau\kappa_6'}{\beta}\right)\int_{t-\tau}^{t}\mu_n^2(s)ds \\
&- \frac{\tau\kappa_6'}{\beta}\int_{t-\tau}^{t}\mu_n^2(s)ds - \left(\frac{1}{\nu_2} - \frac{\tau\kappa_7'}{\beta}\right)\int_{t-\tau}^{t}\mu_{n-1}^2(s)ds \\
&- \frac{\tau\kappa_7'}{\beta}\int_{t-\tau}^{t}\mu_{n-1}^2(s)ds + \frac{\tau}{\beta}\kappa_4' + d^{*2} + \frac{\tau}{\beta}\kappa_5' \\
\le &-\sum_{i=1}^{n}\hat{h}_i\mu_i^2 - \left(\frac{1}{\tau} - \frac{m\beta}{2}\right)\frac{1}{\beta}\int_{t-\tau}^{t}\int_{\theta}^{t}||\dot{v}(s)||^2 dsd\theta \\
&- \left(\frac{1}{\tau} - \frac{\nu_1\kappa_6'}{\beta}\right)\frac{1}{\nu_1}\int_{t-\tau}^{t}\int_{\theta}^{t}\mu_n^2 dsd\theta - \frac{\tau\kappa_6'}{\beta}\int_{t-\tau}^{t}\mu_n^2(s)ds \\
&- \left(\frac{1}{\tau} - \frac{\nu_2\kappa_7'}{\beta}\right)\frac{1}{\nu_2}\int_{t-\tau}^{t}\int_{\theta}^{t}\mu_{n-1}^2 dsd\theta - \frac{\tau\kappa_7'}{\beta}\int_{t-\tau}^{t}\mu_{n-1}^2(s)ds \\
&+ \frac{\tau}{\beta}\kappa_4' + d^{*2} + \frac{\tau}{\beta}\kappa_5' \\
\le &-\varrho V_\mu + \kappa
\end{aligned} \tag{96}$$

where $\varrho = \min\{2\hat{h}_i, \frac{1}{\tau} - \frac{m\beta}{2}, \frac{1}{\tau} - \frac{\nu_1\kappa_6'}{\beta}, 1, \frac{1}{\tau} - \frac{\nu_2\kappa_7'}{\beta}, \quad i = 1, 2, \cdots, n\}$ and $\kappa = \frac{\tau}{\beta}\kappa_4' + d^{*2} + \frac{\tau}{\beta}\kappa_5'$.

By integrating (96) on both sides over [0, t], one can obtain that

$$V_\mu(t) \le (V_\mu(0) - \frac{\kappa}{\varrho})e^{-\varrho t} + \frac{\kappa}{\varrho} \tag{97}$$

From (98), we can conclude that μ_i is bounded, i.e.,

$$|\mu_i| \le \sqrt{2(V_\mu(0) - \kappa/\varrho)e^{-\varrho t} + \kappa/\varrho} \quad i = 1, 2, \cdots, n. \tag{98}$$

According to (78), the signals z_i, $\tilde{W}_i$, γ_i, $\tilde{D}_i$ and e_{i+1} for $1 \le i \le n$ are all bounded. Furthermore, from (17), (39), (61) and (98) one can get α_i and v are also bounded. Thus,

ω_i is bounded which can be derived from the fact that e_{i+1} and α_i. Consequently, based on the boundedness of z_i, μ_i, ω_i, α_i and v, one can get x_i is also bounded. In particular, one can get $|y - y_d| \leq |z_1| + |\mu_1|$ which means that the tracking error is bounded. From above discussions, we can get that for $1 \leq i \leq n$, all the signals of the closed-loop system are all bounded. The proof is completed.

Remark 5 From above discussions, the tracking error can be minimized by adjusting the design parameters k_i, h_i, g_i, σ_i, p_i, l_i and ξ_i, such that a good robust performance of the closed-loop systems can be obtained. In particular, if we increase the parameters k_i, h_i, g_i, p_i and l_i, the tracking errors will be decreased. On the other hand, if we decrease the parameters of ξ_i, σ_i, then the tracking errors will also be decreased.

Remark 6 Based on the auxiliary system, the disturbance observer is introduced to estimate the approximation error and unknown time-varying external disturbance. There is no need to know the boundary of the approximation error or time-varying external disturbance.

Remark 7 The output information of the disturbance observer is employed to construct the virtual control signal and the real control signal. Then the control signal can be adaptive adjusted according to the output of the disturbance observer. Compared with the existing results in [28–33, 49–53], the proposed adaptive neural dynamic surface control scheme in this paper which not only estimates the unknown time-varying external disturbance and the approximation error caused by the NNS, but also eliminates the effect caused by input delay and dead-zone. Consequently, the disturbance rejection performance of the closed-loop system can be effectively improved.

Remark 8 In practical applications, the proposed auxiliary system can be constructed easily according to the number of system state variables. The compensation signal $\mu_i(\mathrm{i} = 1, 2, \cdots, \mathrm{n})$ in the auxiliary system can be used in the virtual signals and real control signal. The stability of the closed-loop system can also be guaranteed by choosing the appropriate Lyapunov function and the setting parameters.

4 Simulation

In this section, two examples of strict-feedback nonlinear systems are given to show the effectiveness and characteristics of the proposed method. Example 1 is a third-order numerical example with constant input delay and dead-zone used for a comparison with the proposed method in [53]. Example 2 is an application example of third-order one-link robot system with time-varying input delay and dead-zone used to show the superiority of the proposed approach.

Example 1 A third-order nonlinear system with time-varying external disturbance, input dead-zone and input delay described as the following form:

$$\begin{cases} \dot{x}_1 = -x_1^2 - sin(x_1) + x_2 + d_1(t) \\ \dot{x}_2 = x_1^2 + x_1 x_2 + x_2 cos(x_1) + x_3 + d_2(t) \\ \dot{x}_3 = 0.1 x_1 x_2 e^{x_3} + 0.5 x_3 \cos(x_1 x_2) + D(v(t-\tau)) + d_3(t) \\ y = x_1 \end{cases}$$

where $d_1(t) = 0.5cos(t)$, $d_2(t) = sin(0.5t)$ and $d_3(t) = sin(0.2t) + 0.5cos(0.1t)$ are time-varying external disturbance. The initial conditions $x(0) = [0.5, 0, 0]^T$.

The control object is to make the output to track the reference signal $y_d = 0.5sin(t) + 0.5cos(0.5t)$ with the input delay being $\tau = 1s$, and the dead-zone parameters being $m = 1$, $b_r = 2$, $b_l = -2$.

Firstly, in order to verify the effectiveness of the proposed method in this paper, a comparison with the proposed method in [53] is carried out to test the tracking performance for the reference signal.

The simulation parameters in [53] (please see [53]) which are selected as $k_1 = 20$, $k_2 = 30$, $k_3 = 40$, $\Lambda_1 = 0.01I$, $\Lambda_2 = 0.02I$, $\Lambda_3 = 0.01I$, $\sigma_1 = 5$, $\sigma_2 = 8$, $\sigma_3 = 15$, $c_1 = 8$, $c_2 = 10$, $c_3 = 15$, $l_1 = 20$, $l_2 = 20$, $l_3 = 50$, $\beta_1 = 0.015$, $\beta_2 = 0.01$. The simulation result is shown in Fig. 1.

From Fig. 1, one can observe that the system trajectory x_1 can not track the reference signal y_d, and the system trajectory x_1 is unstable when the input delay $\tau = 1s$, input dead-zone, and external disturbances appear. The simulation result shows that the control signal is completely invalid when the input delay occurs. This means that, the Pade approximation method is invalid for long input delay.

In what follows, we test the effectiveness of the proposed method in this article. In the simulation, some parameters are selected as above, let the parameters be $\hat{W}_1(0) = \hat{W}_2(0) = \hat{W}_3(0) = 0.1$, $\gamma_1(0) = \gamma_2(0) = \gamma_3(0) = 0$, $\mu_1(0) = \mu_2(0) = \mu_3(0) = 0$, $\omega_1(0) = \omega_2(0) = 0$, $o_1(0) = o_2(0) = o_3(0) = 0$, $k_1 = 20$, $k_2 = 30$, $k_3 = 40$, $h_1 = 2$, $h_2 = 4$, $h_3 = 3$, $g_1 = 1$, $g_2 = 1$, $\Lambda_1 = 0.01I$, $\Lambda_2 = 0.02I$, $\Lambda_3 = 0.01I$, $\sigma_1 = 5$, $\sigma_2 = 8$, $\sigma_3 = 15$, $p_1 = 8$, $p_2 = 10$, $p_3 = 15$, $l_1 = 20$, $l_2 = 20$, $l_3 = 50$, $\xi_1 = 0.015$, $\xi_2 = 0.01$. The Gaussian NNS are employed in the

simulation, and the center of the receptive field is $v = [-5,-4,-3,-2,-1,0,1,2,3,4,5]^T$ with the width $\eta = 1$. The simulation time is $30s$, and the simulation results are shown in Figs. 2, 3, 4, 5, 6, 7, 8, 9, 10.

Figure 2 draws the trajectories of the state x_1 and y_d.

From Fig. 2, one can observe that under the input delay $\tau = 1s$, input dead-zone and external disturbances, the system state trajectory of x_1 can track y_d quickly.

Figure 3 draws the state trajectories of x_2 and x_3, respectively. From Fig.3 one can observe that the state trajectories of x_2 and x_3 are all bounded with input delay $\tau = 1s$, input dead-zone, and time-varying external disturbances.

Figure 4 depicts the trajectories of z_1, z_2 and z_3 are all bounded with input delay $\tau = 1s$, input dead-zone and time-varying external disturbances. This means that the proposed adaptive controller can ensure that the tracking errors converge to a compact set of the origin.

Figure 5 depicts the state trajectories of auxiliary system μ_1, μ_2 and μ_3

From Fig. 5, one can observe that the auxiliary systems μ_1, μ_2 and μ_3 are asymptotically stable. Therefore, the compensation signals are bounded, which verifies the correctness of the theoretical analysis.

Figure 6 displays the adaptive laws $\hat{W}_1$, $\hat{W}_2$ and $\hat{W}_3$ are bounded.

From the simulation result in Fig.6, although the input delay and input dead zone exist in practical system, one can conclude that the adaptive laws are all bounded. This demonstrates the effectiveness of the proposed compensation mechanism.

Figures 7, 8 and 9 depict the trajectories of $\hat{D}_1$, D_1, $\hat{D}_2$, D_2, $\hat{D}_3$, D_3, respectively.

From Figs. 7, 8, 9, one can observe that the proposed disturbance observer can estimate the approximation error and the external time-varying disturbance accurately and quickly. This means that the proposed disturbance observer can effectively provide the estimation information for the adaptive controller, thus improving the disturbance rejection performance of the closed-loop system.

The control signal $D(v(t-\tau))$ with $\tau = 1s$ is shown in Fig. 10. It can be seen from Fig. 10 that the input signal is bounded.

From Fig. 10, one can observe that the proposed controller is bounded by using the compensation mechanism, although the input delay and input dead zone exist in practical system.

From the simulation results in Figs. 2, 3, 4, 5, 6, 7, 8, 9, 10 one can obtain that for input delay $\tau = 1s$ and the time-varying external disturbance $d_1(t) = 0.5cos(t)$, $d_2(t) = sin(0.5t)$ and $d_3(t) = sin(0.2t) + 0.5cos(0.1t)$, and input dead-zone, all the signals of the closed-loop systems are bounded by using the proposed adaptive neural controller.

From the comparative results of Figs. 1, 2, 3, 4, 5, 6, 7, 8, 9, 10, one can observe that the proposed method in this paper can tackle disturbance-observer-based adaptive control for strict-feedback systems with long input delay and dead-zone. At the same time, the proposed scheme shows excellent tracking performance.

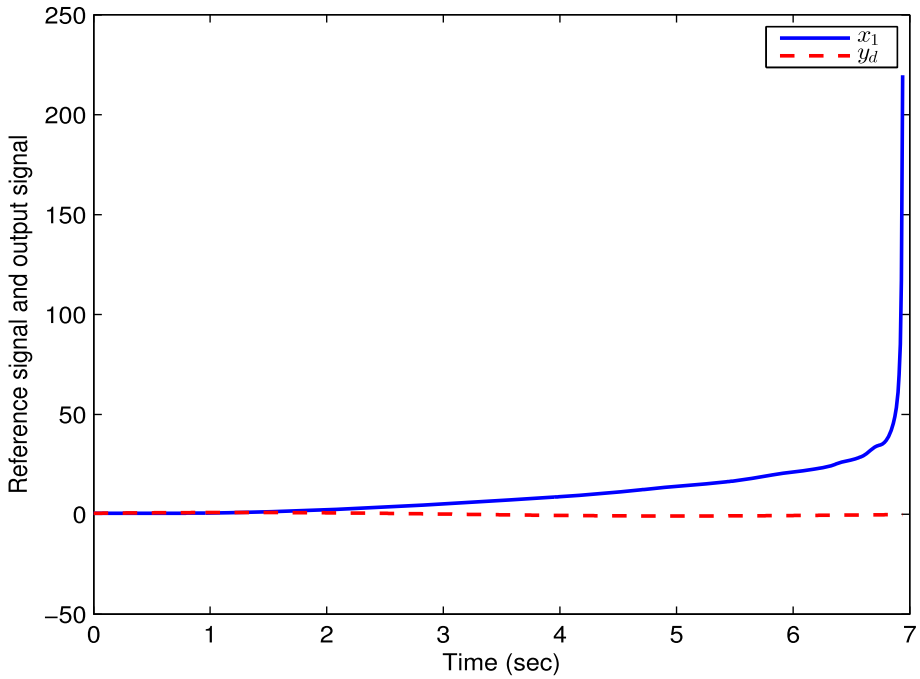

Fig. 1 The trajectories of x_1 and y_d with input delay $\tau = 1s$ using the method [53] in example 1

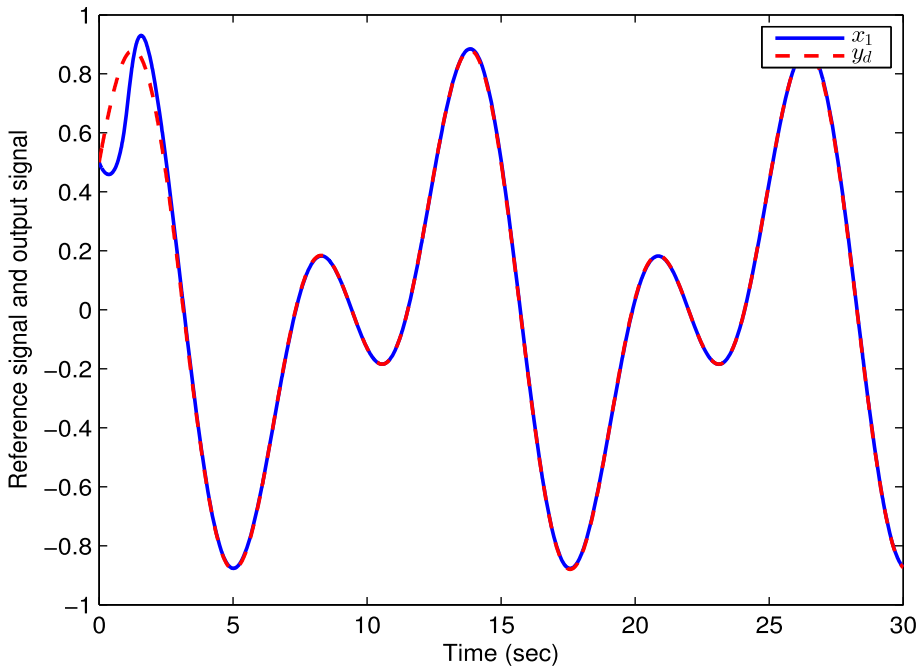

Fig. 2 The trajectories of x_1 and y_d with input delay $\tau = 1s$ in example 1

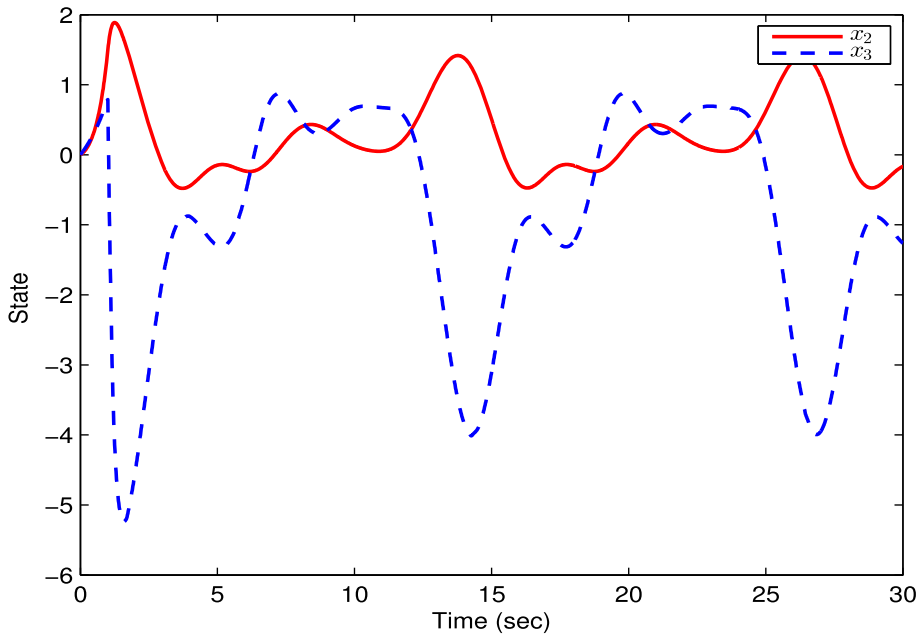

Fig. 3 The trajectories of x_2 with input delay $\tau = 1s$ in example 1

Example 2 Consider a one-link robot system used in [58]. The dynamics model of the system with input dead-zone and time-varying delay is described as follows:

$$\begin{cases} D\ddot{q} + B\dot{q} + N\sin(q) = I \\ M\dot{I} + JI = -K_m\dot{q} + D(v(t-\tau)) \\ y = q \end{cases}$$

where q represents the link position, $\dot{q}$ represents the angular velocity, and $\ddot{q}$ represents the angular acceleration. I denotes the motor shaft angle and $\dot{I}$ denotes the velocity. v is the motor torque, and $D(v(t-\tau))$ represents the input dead-zone and delay for control input v.

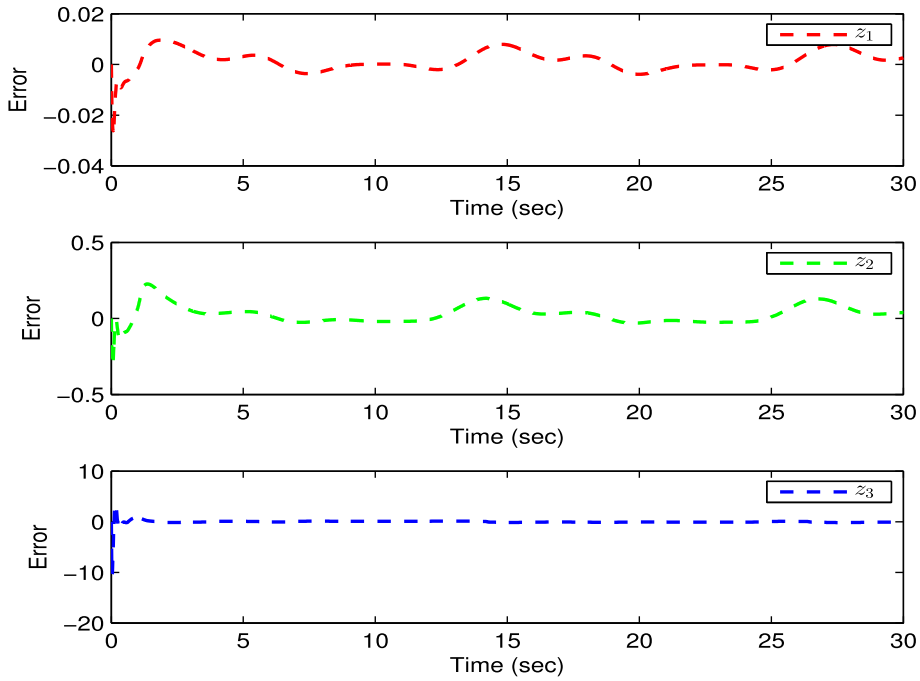

Fig. 4 The trajectories of z_1,z_2 and z_3 in example 1

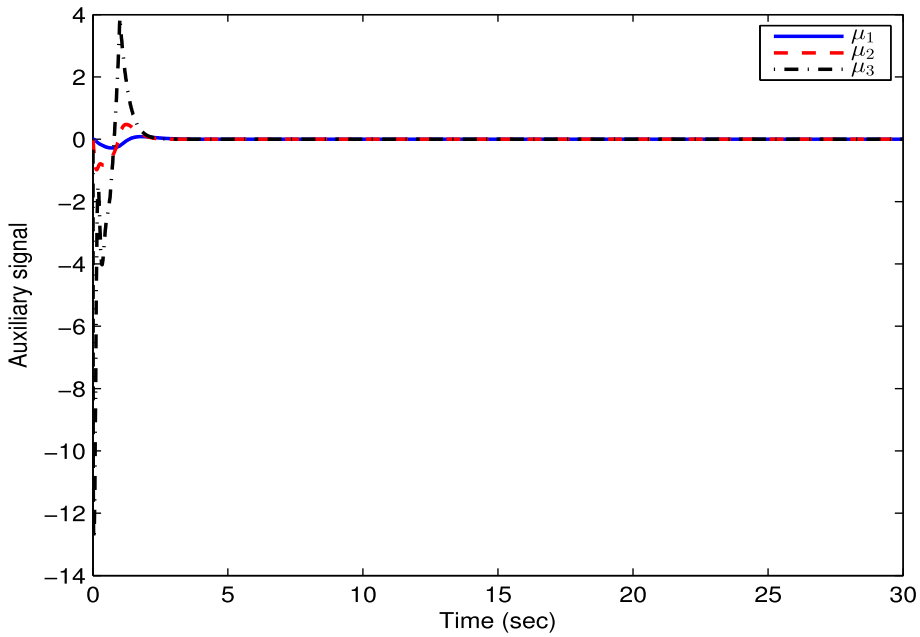

Fig. 5 The auxiliary system's states μ_1, μ_2 and μ_3 in example 1

Let $x_1 = q$, $x_2 = \dot{q}$ and $x_3 = I/D$, we add the external disturbances $d_1(t) = 0.3sin(t)$, $d_2(t) = 0.2sin(2t)$ and $d_3(t) = 0.3cos(t)$ and rewrite the system as

$$\begin{cases} \dot{x_1} = x_2 + d_1(t) \\ \dot{x_2} = -\dfrac{N}{D}\sin(x_1) - \dfrac{B}{D}x_2 + x_3 + d_2(t) \\ \dot{x_3} = -\dfrac{K_m}{M}x_2 - \dfrac{DJ}{M}x_3 + \dfrac{1}{M}D(v(t-\tau)) + d_3(t) \\ y = x_1 \end{cases}$$

where $D = 1$, $B = 1$, $M = 1$, $K_m = 10$, $J = 0.5$, $N = 10$ and $x(0) = [0, 0, 0]^T$.

The control object is to make the output to track the reference signal $y_d = 0.5sin(t)$ with the time-varying input delay being $\tau = 0.8 + 0.5sin(t)s$, and the dead-zone parameters being $m = 2.5$, $b_r = 2$, $b_l = -2$.

Let the initial conditions $\hat{W}_1(0)= \hat{W}_2(0)= \hat{W}_3(0) = 0.01$, $\gamma_1(0) = \gamma_2(0) = \gamma_3(0) = 0$, $\mu_1(0)=\mu_2(0)=\mu_3(0) = 0$, $\omega_1(0) = \omega_2(0) = 0$,

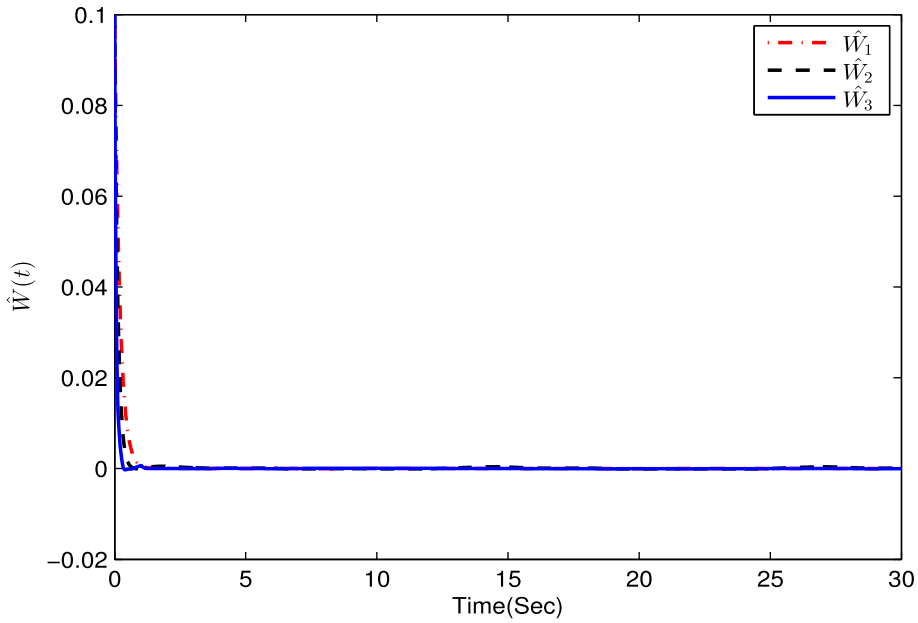

Fig. 6 The adaptive laws' trajectories $\hat{W}_1$, $\hat{W}_2$ and $\hat{W}_3$ in example 1

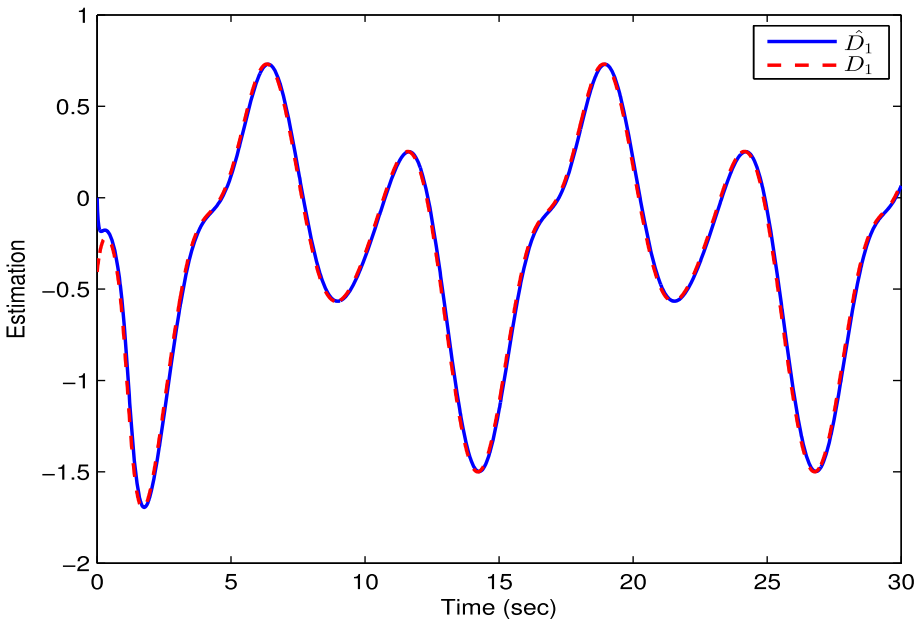

Fig. 7 The adaptive laws' trajectories $\hat{D}_1$, and D_1 in example 1

$o_1(0) = o_2(0) = o_3(0) = 0$, $k_1 = 20$, $k_2 = 10$, $k_3 = 10$, $h_1 = 8$, $h_2 = 8$, $h_3 = 5$, $g_1 = 2$, $g_2 = 2$, $\Lambda_1 = 0.0001I$, $\Lambda_2 = 0.0001I$, $\Lambda_3 = 0.0001I$, $\sigma_1 = 1$, $\sigma_2 = 1$, $\sigma_3 = 1$, $p_1 = 9$, $p_2 = 9$, $p_3 = 9$, $l_1 = 18$, $l_2 = 18$, $l_3 = 18$, $\xi_1 = 0.015$, $\xi_2 = 0.01$. The Gaussian NNS are employed in the simulation, and the center of the receptive field is $v = [-5, -4, -3, -2, -1, 0, 1, 2, 3, 4, 5]^T$ with the width $\eta = 1$. The simulation time is $30s$, and the simulation results are shown in Figs. 11, 12, 13, 14, 15, 16, 17, 18, 19. The trajectories of the state x_1 and y_d are depicted in Fig. 11.

From Fig. 11, one can observe that under the input delay $\tau = 0.8 + 0.5sin(t)s$, input dead-zone and external disturbances, the system state trajectory of x_1 can track the reference signal y_d.

Figure 12 draws the state trajectories of x_2 and x_3.

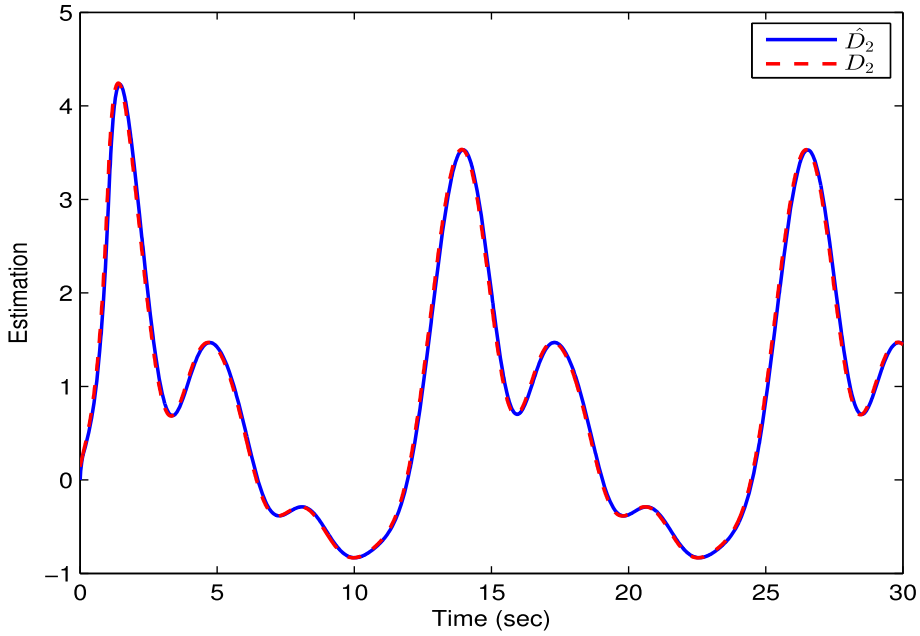

Fig. 8 The adaptive laws' trajectories $\hat{D}_2$, and D_2 in example 1

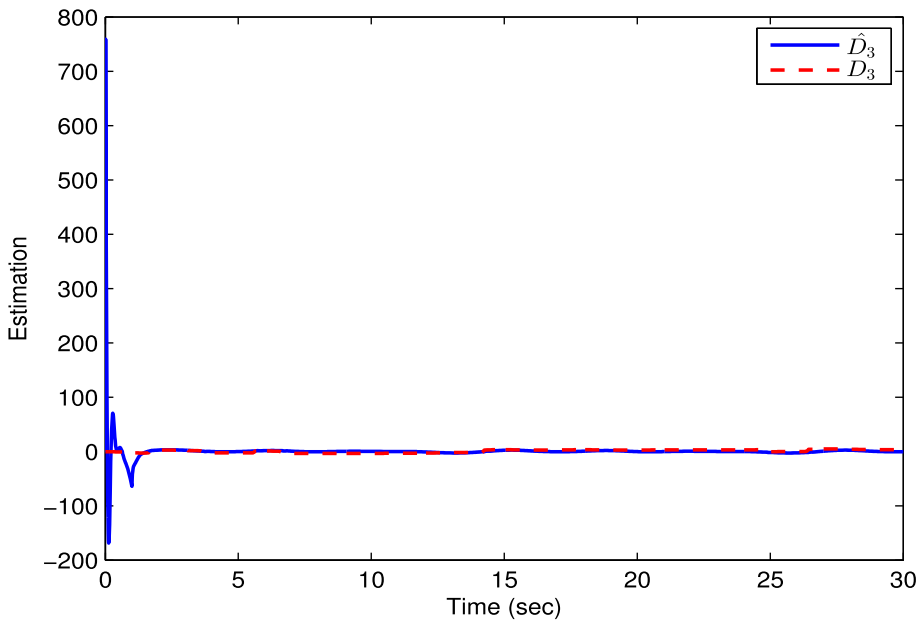

Fig. 9 The adaptive laws' trajectories $\hat{D}_3$, and D_3 in example 1

From Fig.12 we can see that the state trajectories of x_2 and x_3 are bounded with input delay $\tau = 0.8 + 0.5sin(t)s$, input dead-zone and external disturbances.

Figure 13 depicts the trajectories of z_1, z_2 and z_3.

From Fig. 13, we can observe that all the signals of the tracking errors are bounded by using the proposed adaptive controller with input delay $\tau = 0.8 + 0.5sin(t)s$, input dead-zone and time-varying external disturbances.

Figure 14 shows the state trajectories of auxiliary system μ_1, μ_2 and μ_3 are asymptotically stable.

Figure 15 displays the adaptive laws $\hat{W}_1$, $\hat{W}_2$ and $\hat{W}_3$ are bounded with time-varying input delay, input dead-zone and time-varying external disturbances.

Figures 16, 17 and 18 depict the trajectories of $\hat{D}_1$, D_1, $\hat{D}_2$, D_2, $\hat{D}_3$, D_3, respectively.

From Figs. 16, 17, 18, one can observe that the proposed disturbance observer can estimate the approximation error and the external time-varying disturbance accurately and quickly.

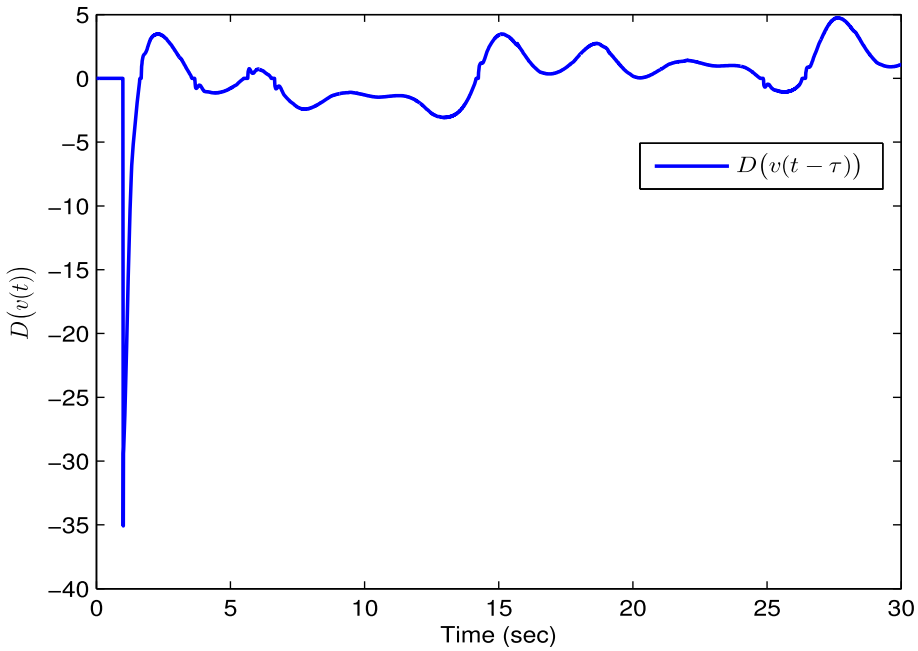

Fig. 10 The control signal $D(v(t-\tau))$ with $\tau = 1s$ in example 1

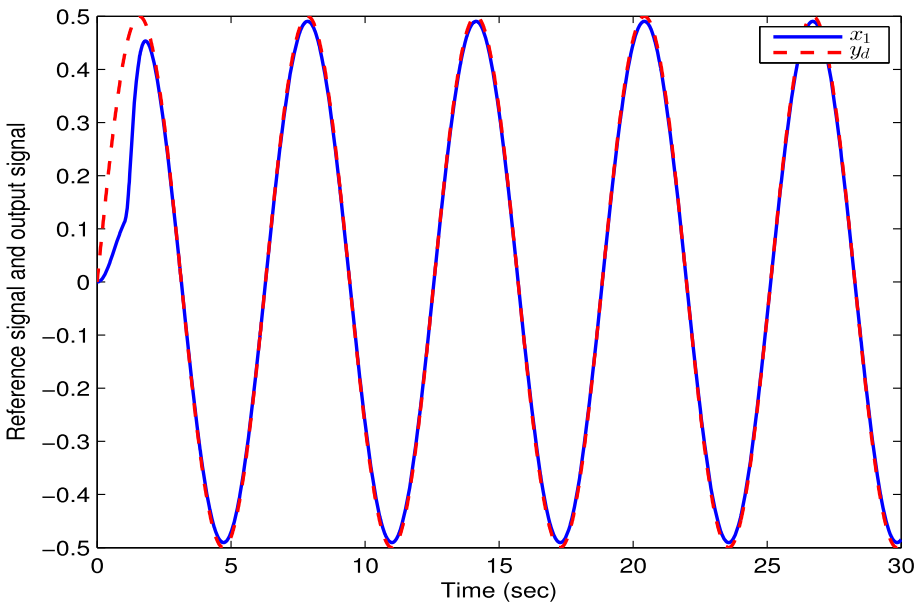

Fig. 11 The trajectories of x_1 and y_d with time-varying input delay $\tau = 0.8 + 0.5sin(t)s$ in example 2

The control signal $D(v(t-\tau))$ with $\tau = 0.8 + 0.5sin(t)s$ is shown in Fig.19.

From the simulation results in Figs. 11, 12, 13, 14, 15, 16, 17, 18, 19, one can conclude that for the time-varying input delay $\tau = 0.8 + 0.5sin(t)s$, input dead-zone and the time-varying external disturbance $d_1(t) = 0.3sin(t)$, $d_2(t) = 0.2sin(2t)$ and $d_3(t) = 0.3cos(t)$, all the signals of the closed-loop systems are bounded by using the proposed adaptive neural controller.

In order to illustrate the superiority of the proposed method in this paper, a comparison with [52] and [53] is carried out to test the effectiveness of the method in handling different input delays. The reference signal is selected as above, and the comparison results are shown in Table 1. In Table 1, the mark ✓ denotes the output signal can track the reference signal, and the mark × denotes the output signal cannot track the reference signal.

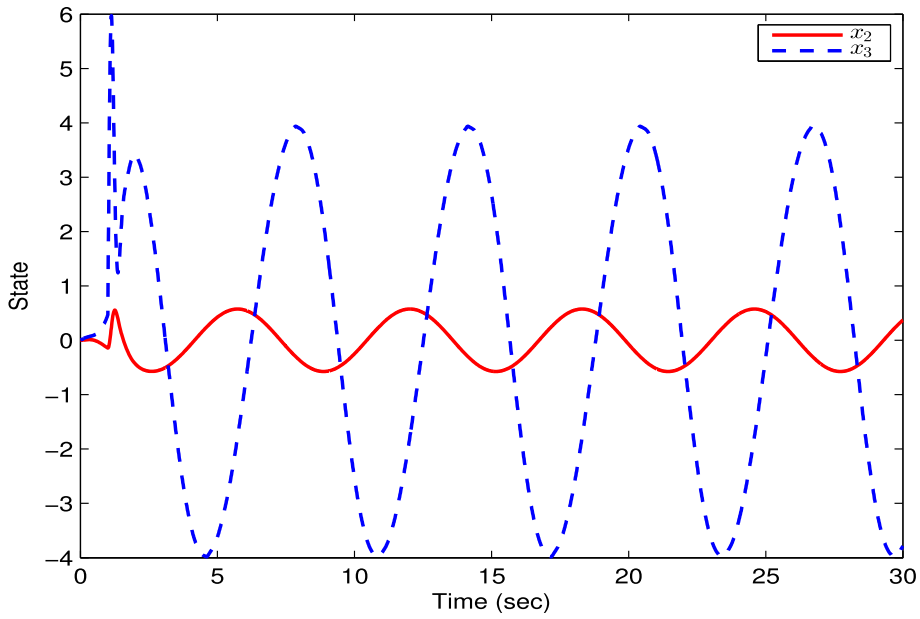

Fig. 12 The state trajectory of x_2 and x_3 with input delay $\tau = 0.8 + 0.5sin(t)s$ in example 2

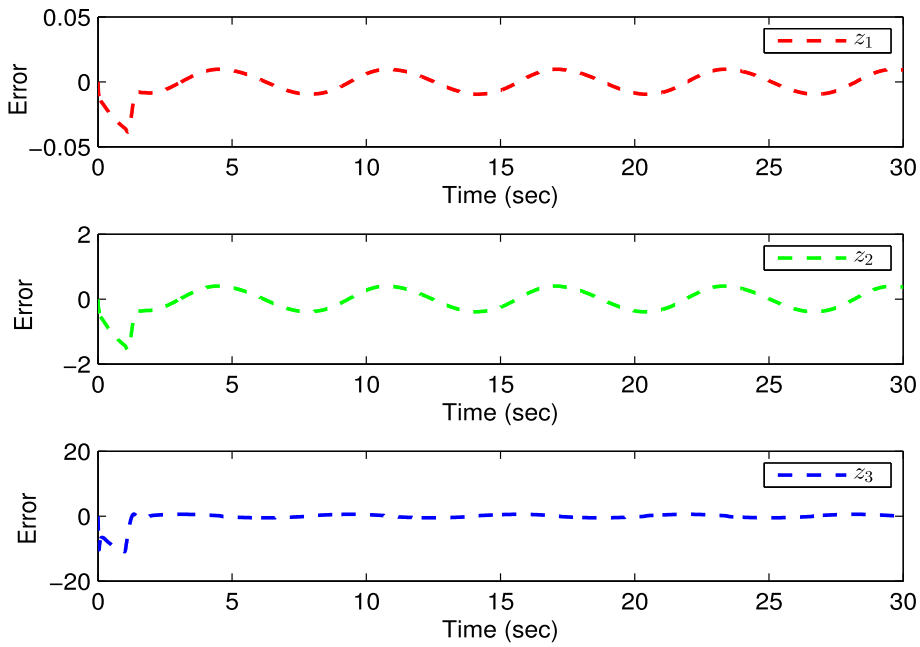

Fig. 13 The trajectory of z_1, z_2 and z_3 in example 2

From the results in Table 1, one can observe that for the smallest input delay, all proposed method are effectiveness. However, if the input delay $\tau \geq 0.1s$, the method in [52] is completely invalid, and the output signal of the system cannot track the reference signal. The method in [53] is superior to the method in [52]. However, if the input delay $\tau \geq 1.5s$, then the closed-loop system become unstable for the method in [53]. For the proposed method in this paper, the system state variables are still controllable when $\tau \leq 2.0s$. From the results in Table 1, one can conclude that the proposed method in this paper is super to the methods in [52, 53].

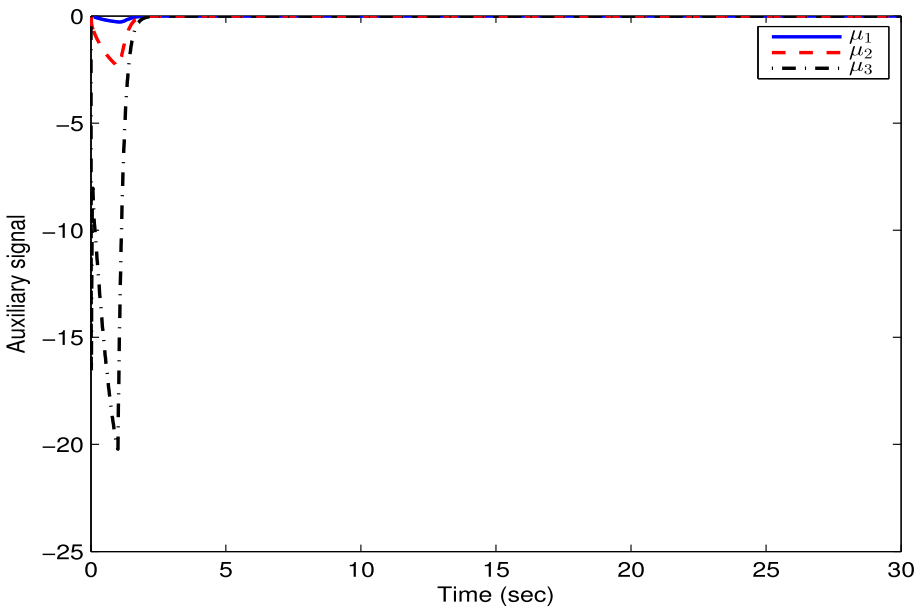

Fig. 14 The auxiliary system's states μ_1, μ_2 and μ_3 in example 2

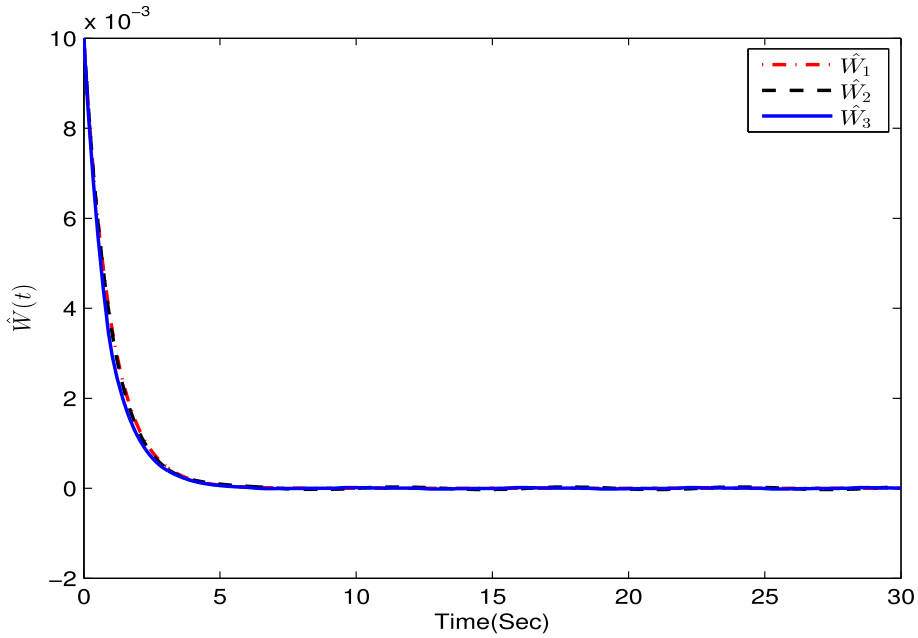

Fig. 15 The adaptive laws' trajectories $\hat{W}_1$, $\hat{W}_2$ and $\hat{W}_3$ in example 2

4.1 Comparative explanations

The proposed method in this paper gives an effective way for strict-feedback nonlinear systems with time-varying external disturbance, input dead-zone and input delay. Compared with the existing results in [13–16, 28–33, 49–53], the main advantages of the proposed method can be summarized in the following three aspects.

(1) The proposed compensation mechanism is convenient to overcome the design difficulty on the input-delay systems theoretically. Unlike the Pade approximation method which is invalid once the input delay is long, the proposed method can tackle long input delay.

(2) Different from [28–33], the proposed control scheme can not only estimate the unknown time-varying external disturbance and the approximation error caused by the NNS, but also eliminate the effect caused by input delay and dead-zone.

(3) Compared with the existing results in [13–16] [49–53], the disturbance rejection performance of

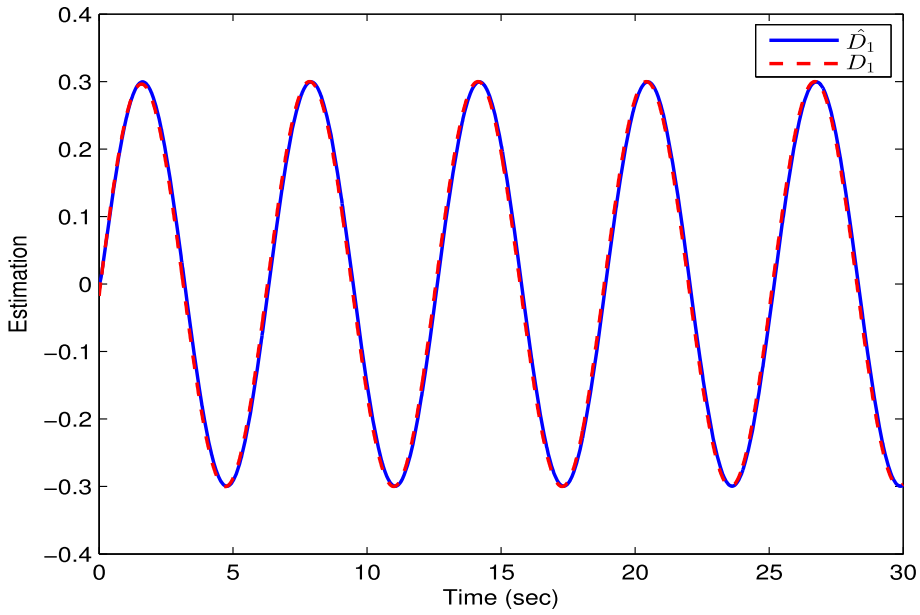

Fig. 16 The adaptive laws' trajectories $\hat{D}_1$, and D_1 in example 1

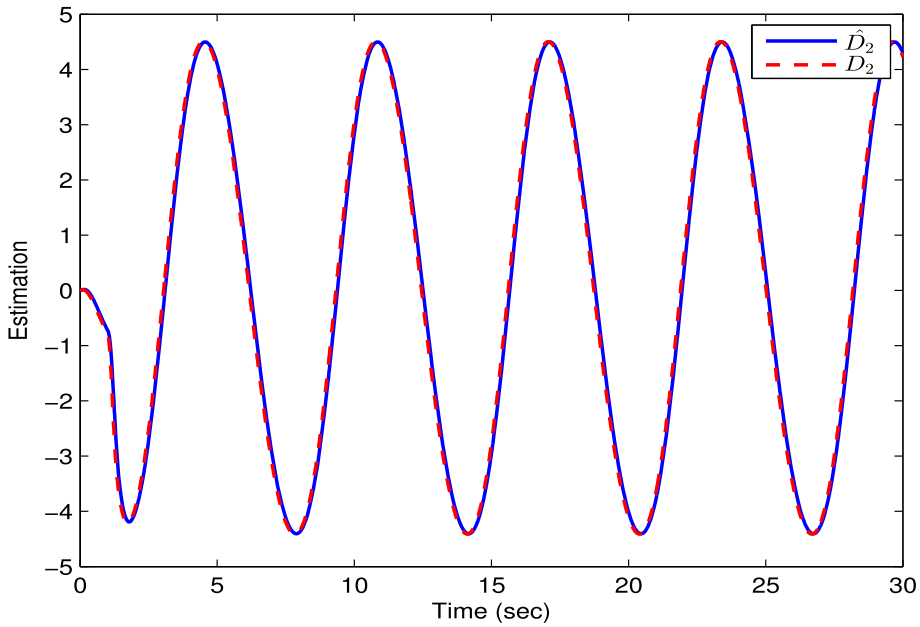

Fig. 17 The adaptive laws' trajectories $\hat{D}_2$, and D_2 in example 1

the closed-loop system can be effectively improved. Especially, when the system has input delay and dead zone, the robust performance of the system can be effectively guaranteed.

5 Conclusions

In this article, based on the idea of DSC scheme and by combing NNS with backstepping technique, we consider disturbance-observer-based adaptive tracking control for strict-feedback nonlinear systems with time-varying external disturbance, input dead-zone and input delay. To degrade the complexity and difficulty of controller design, a novel compensation mechanism is developed to exclude the effect caused by input dead-zone and input delay. Based on the auxiliary system, a disturbance observer is constructed to estimate the approximation error and the unknown external time-varying disturbance in each back-stepping step, and the effect of input dead zone and delay can be eliminated. The "explosion of complexity" problem has been avoided by DSC scheme. Finally, the simulation

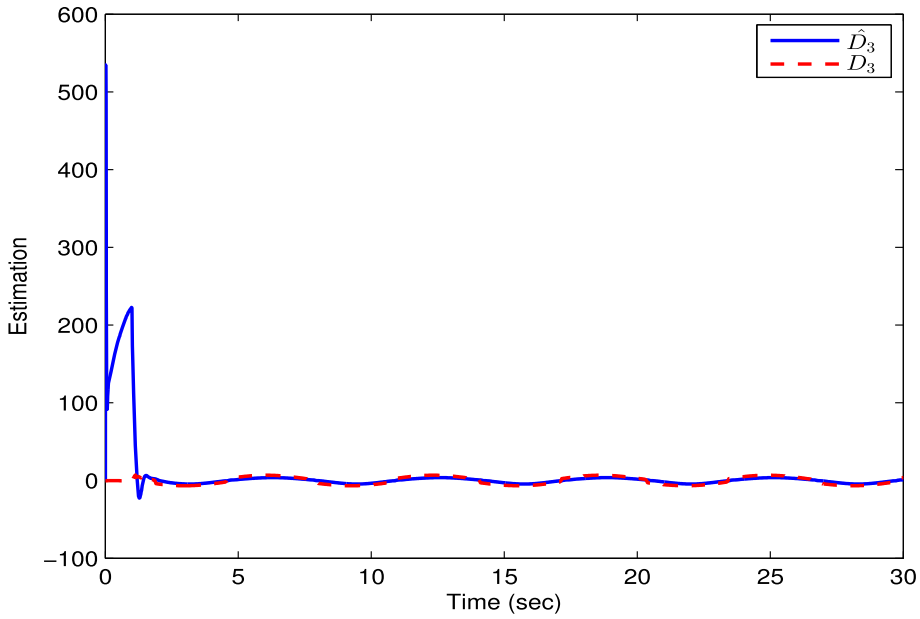

Fig. 18 The adaptive laws' trajectories $\hat{D}_3$, and D_3 in example 1

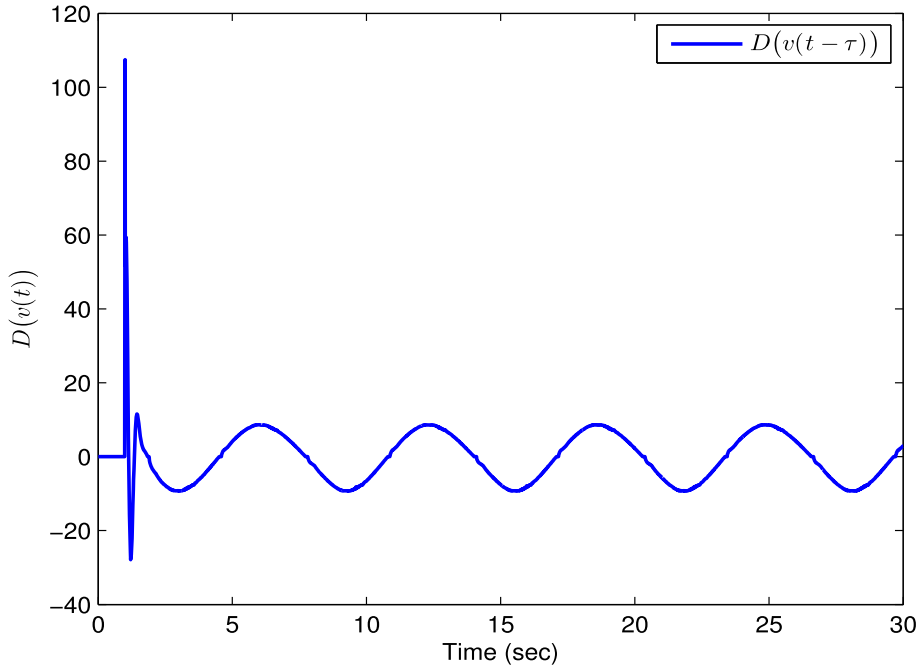

Fig. 19 The control signal $D(v(t-\tau))$ with $\tau = 0.8 + 0.5sin(t)s$ in example 2

Table 1 The comparison between different methods

	$\tau = 0.02s$	$\tau = 0.1s$	$\tau = 1.0s$	$\tau = 1.5s$	$\tau = 2.0s$	$\tau = 3.0s$
[52]	✓	×	×	×	×	×
[53]	✓	✓	✓	×	×	×
This paper	✓	✓	✓	✓	✓	×

results show that the proposed scheme has better tracking performance. In the future, we will discuss the problem of nonlinear systems control with unknown input delay in depth.

Acknowledgements This research was financially supported by the National Natural Science Foundation of China (Grants Nos. 11871117 and 61873041).

Declarations

Conflict of interest The authors declare that there is no conflict of interests regarding the publication of this paper.

References

1. Mayne D (2002) Nonlinear and adaptive control design. IEEE Trans Autom Contr 41(12):1849
2. Chang XH, Xiong J, Li ZM et al (2017) Quantized static output feedback control for discrete-time systems. IEEE Trans Ind Info 14(8):3426–3435
3. Zou W, Shi P, Xiang Z et al (2020) Finite-time consensus of second-order switched nonlinear multi-agent systems. IEEE Trans Neur Netw Learn Sys 31(5):1757–1762
4. Qi W, Gao X, Ahn CK et al (2022) Fuzzy integral sliding-mode control for nonlinear semi-Markovian switching systems with application. IEEE Trans Sys, Man Cybern: Sys 52(3):1674–1683
5. Li S, Ahn CK, Xiang Z (2019) Sampled-data adaptive output feedback fuzzy stabilization for switched nonlinear systems with asynchronous switching. IEEE Trans Fuzzy Sys 27(1):200–205
6. Tong S, Min X, Li Y (2020) Observer-based adaptive fuzzy tracking control for strict-feedback nonlinear systems with unknown control gain functions. IEEE Trans Cybern 50(9):3903–3913
7. Wang X, Niu B, Song X et al (2021) Neural networks-based adaptive practical preassigned finite-time fault tolerant control for nonlinear time-varying delay systems with full state constraints. Int J Rob Nonlin Contr 31(5):1497–1513
8. Liu Y, Zhu Q, Wen G (2022) Adaptive Tracking Control for Perturbed Strict-Feedback Nonlinear Systems Based on Optimized Backstepping Technique. IEEE Trans Neur Netw Learn Sys 33(2):853–865
9. Wang H, Liu PX, Xie X et al (2021) Adaptive fuzzy asymptotical tracking control of nonlinear systems with unmodeled dynamics and quantized actuator. Info Sci 575:779–792
10. Li Y, Liu Y, Tong S (2021) Observer-based neuro-adaptive optimized control of strict-feedback nonlinear systems with state constraints. IEEE Trans Neur Netw Learn Sys. https://doi.org/10.1109/TNNLS.2021.3087796
11. Swaroop D, Gerdes JC, Yip PP et al (1997) Dynamic surface control of nonlinear systems. Am Contr Conf 5:3028–3034
12. Chen M, Tao G, Jiang B (2014) Dynamic surface control using neural networks for a class of uncertain nonlinear systems with input saturation. IEEE Trans Neur Netw Learn Sys 26(9):2086–2097
13. Wang H, Xu K, Liu PX et al (2021) Adaptive fuzzy fast finite-time dynamic surface tracking control for nonlinear systems. IEEE Trans Circ Sys I: Regular Pap 68(10):4337–4348
14. Ma Z, Ma H (2019) Adaptive fuzzy backstepping dynamic surface control of strict-feedback fractional-order uncertain nonlinear systems. IEEE Trans Fuzzy Sys 28(1):122–133
15. Sun K, Liu L, Qiu J et al (2021) Fuzzy adaptive finite-time fault-tolerant control for strict-feedback nonlinear systems. IEEE Trans Fuzzy Sys 29(4):786–796
16. Zhao J, Li X, Tong S (2020) Fuzzy adaptive dynamic surface control for strict-feedback nonlinear systems with unknown control gain functions. Int J Sys Sci 1:1–16
17. Sun K, Qiu J, Karimi HR et al (2021) Event-triggered robust fuzzy adaptive finite-time control of nonlinear systems with prescribed performance. IEEE Trans Fuzzy Sys 29(6):1460–1471
18. Yan X, Chen M, Feng G et al (2019) Fuzzy robust constrained control for nonlinear systems with input saturation and external disturbances. IEEE Trans Fuzzy Sys 29(2):345–356
19. Min H, Xu S, Fei S et al (2021) Observer-based NN control for nonlinear systems with full-state constraints and external disturbances. IEEE Trans Neur Netw Learn Sys. https://doi.org/10.1109/TNNLS.2021.3056524
20. Li K, Tong S (2019) Fuzzy adaptive practical finite-time control for time delays nonlinear systems. Int J Fuzzy Sys 21(4):1013–1025
21. Liu Y, Liu X, Jing Y et al (2019) Direct adaptive preassigned finite-time control with time-delay and quantized input using neural network. IEEE Trans Neur Netw Learn Sys 31(4):1222–1231
22. Wang H, Kang S, Zhao X et al (2021) Command filter-based adaptive neural control design for nonstrict-feedback nonlinear systems with multiple actuator constraints. IEEE Trans Cybern. https://doi.org/10.1109/TCYB.2021.3079129
23. Xu Q, Wang Z, Zhen Z (2019) Adaptive neural network finite time control for quadrotor UAV with unknown input saturation. Nonlin Dyn 98(3):1973–1998
24. Nakao M, Ohnishi K, Miyachi K (1987) A robust decentralized joint control based on interference estimation. IEEE Int Conf Robot Automat 4:326–331
25. Xu B, Zhang L, Ji W (2021) Improved non-singular fast terminal sliding mode control with disturbance observer for PMSM drives. IEEE Trans Transport Electrif 7(4):2753–2762
26. Liu X, Yu H (2021) Continuous adaptive integral-type sliding mode control based on disturbance observer for PMSM drives. Nonli Dyn 104(2):1429–1441
27. Zhang J, Liu X, Xia Y et al (2016) Disturbance observer-based integral sliding-mode control for systems with mismatched disturbances. IEEE Trans Ind Electr 63(11):7040–7048
28. Zhang H, Wei X, Zhang L et al (2017) Disturbance rejection for nonlinear systems with mismatched disturbances based on disturbance observer. J Frankl Instit 354(11):4404–4424
29. Wei XJ, Wu ZJ, Karimi HR (2016) Disturbance observer-based disturbance attenuation control for a class of stochastic systems. Automatica 63:21–25
30. Wei XJ, Dong L, Zhang H et al (2019) Adaptive disturbance observer-based control for stochastic systems with multiple heterogeneous disturbances. Int J Robust Nonlin Contr 29(16):5533–5549
31. Zhao Z, Ren Y, Mu C et al (2021) Adaptive neural-network-based fault-tolerant control for a flexible string with composite disturbance observer and input constraints. IEEE Trans Cybern. https://doi.org/10.1109/TCYB.2021.3090417
32. Qiu J, Wang T, Sun K et al (2022) Disturbance observer-based adaptive fuzzy control for strict-feedback nonlinear systems with finite-time prescribed performance. IEEE Trans Fuzzy Sys 30(4):1175–1184
33. Chen M, Tao G, Jiang B (2015) Dynamic surface control using neural networks for a class of uncertain nonlinear systems with input saturation. IEEE Trans Neur Netw Learn Sys 26:2086–2097
34. Buscarino A, Fortuna CFL, Frasca M (2016) Passive and active vibrations allow self-organization in large-scale electromechanical systems. Int J Bifurcat Chaos 26(07):1650123
35. Bucolo M, Buscarino A, Famoso C et al (2019) Control of imperfect dynamical systems. Nonlin Dyn 98(4):2989–2999
36. Bucolo M, Buscarino A, Famoso C et al (2021) Imperfections in integrated devices allow the emergence of unexpected strange attractors in electronic circuits. IEEE Access 9:29573–29583
37. Tao G, Kokotovic PV (1994) Adaptive control of plants with unknown dead-zones. IEEE Trans Autom Contr 39(1):59–68
38. Wang XS, Su CY, Hong H (2004) Robust adaptive control of a class of nonlinear systems with unknown dead-zone. Automatica 40(3):407–413

39. Zhou Q, Zhao S, Li H et al (2019) Adaptive Neural Network Tracking Control for Robotic Manipulators With dead-zone. IEEE Trans Neur Netw Learn Sys 30(12):3611–3620
40. Wang S, Yu H, Yu J et al (2020) Neural-network-based adaptive funnel control for servo mechanisms with unknown dead-zone. IEEE Trans Cybern 50(4):1383–1394
41. Yu J, Shi P, Dong W, Lin C (2018) Adaptive fuzzy control of nonlinear systems with unknown dead zones based on command filtering. IEEE Trans Fuzzy Sys 26(1):46–55
42. Espitia N, Perruquetti W (2021) Predictor-feedback prescribed-time stabilization of LTI systems with input delay. IEEE Trans Autom Contr 67(6):2784–2799
43. Zhou Y, Wang X, Xu R (2022) Command-filter-based adaptive neural tracking control for a class of nonlinear MIMO state-constrained systems with input delay and saturation. Neur Netw 147:152–162
44. Zhang J, Li S, Ahn CK et al (2022) Decentralized event-triggered adaptive fuzzy control for nonlinear switched large-scale systems with input delay via command-filtered backstepping. IEEE Trans Fuzzy Sys 30(6):2118–2123
45. Li H, Liu Q, Feng G et al (2021) Leader-follower consensus of nonlinear time-delay multiagent systems: A time-varying gain approach. Automatica 126:109444
46. Li X, Li P (2021) Stability of time-delay systems with impulsive control involving stabilizing delays. Automatica 124:109336
47. Liu G, Hua C, Liu PX et al (2021) Input-to-state stability for time-delay systems with large delays. IEEE Trans Cybern. https://doi.org/10.1109/TCYB.2021.3106793
48. Sun J, Yang J, Zeng Z (2022) Predictor-based periodic event-triggered control for nonlinear uncertain systems with input delay. Automatica 136:110055
49. Li H, Wang L, Du H et al (2017) Adaptive fuzzy backstepping tracking control for strict-feedback systems with input delay. IEEE Trans Fuzzy Sys 25(3):642–652
50. Li D, Liu Y, Tong S et al (2019) Neural networks-based adaptive control for nonlinear state constrained systems with input delay. IEEE Trans Cybern 49(4):1249–1258
51. Ma J, Xu S, Cui G et al (2019) Adaptive backstepping control for strict-feedback non-linear systems with input delay and disturbances. IET Contr Theory Appl 13(4):506–516
52. Ma J, Xu S, Li Y et al (2018) Neural networks-based adaptive output feedback control for a class of uncertain nonlinear systems with input delay and disturbances. J Frankl Instit 355(13):5503–5519
53. Zhang Q, Dong J (2020) Disturbance-observer-based adaptive fuzzy control for nonlinear state constrained systems with input saturation and input delay. Fuzzy Sets Sys 392:77–92
54. Sun H, Li S, Yang J et al (2015) Global output regulation for strict-feedback nonlinear systems with mismatched nonvanishing disturbances. Int J Robust Nonlin Contr 25(15):2631–2645
55. Sun Y, Xu J, Lin G et al (2021) Adaptive neural network control for maglev vehicle systems with time-varying mass and external disturbance. Neur Comput Appl. https://doi.org/10.1007/s00521-021-05874-2
56. Sun Y, Xu J, Chen C et al (2022) Reinforcement learning-based optimal tracking control for levitation system of maglev vehicle with input time delay. IEEE Trans Instrument Measur 71:1–13
57. Wang D, Huang J (2005) Neural network-based adaptive dynamic surface control for a class of uncertain nonlinear systems in strict-feedback form. IEEE Trans Neural Netw 16(1):195–202
58. Wang M, Wang C, Shi P et al (2016) Dynamic learning from neural control for strict-feedback systems with guaranteed pre-defined performance. IEEE Trans Neur Netw Learn Sys 27(12):2564–2576